Rep. Prog. Phys. 54 (1991) 949–1003. Printed in the UK

The conditions for the synthesis of heavy nuclei

K-H Schmidt† and W Morawek‡

† Gesellschaft für Schwerionenforschung mbH, D-6100 Darmstadt, Federal Republic of Germany
‡ Institut für Kernphysik, Technische Hochschule, D-6100 Darmstadt, Federal Republic of Germany

We dedicate this work to Professor Peter Armbruster on the occasion of his 60th birthday.

Abstract

In parallel to the attempts to synthesize the heaviest nuclei, systematic studies have been made to obtain better understanding of the reaction aspects. The most comprehensive data have been taken for nearly mass-symmetric massive systems. They combine high Coulomb forces in the entrance channel with evaporation-residue cross sections which are high enough to be easily detectable. With these systems, rather cold compound nuclei can be produced, and even radiative fusion was observed. While one of the most salient features of the thoroughly studied fusion of light and medium-heavy systems is the enhanced sub-barrier fusion, the massive systems exhibit a considerable deficit of fusion above the expected potential barrier. This hindrance to fusion may be attributed to the dynamical evolution of the composite system which may lead to immediate reseparation. The experimental data reveal that the hindrance to fusion is strongly influenced by the nuclear structure of the reaction partners.

The high fission competition in the evaporation cascade of fissile excited compound systems as deduced from measured evaporation-residue cross sections is compared with the expectations of the statistical model. Experimental evidence is presented that the increase of the fission barriers due to spherical shell effects in the ground state does not reduce the fission probability in the de-excitation process. A re-examination of the nuclear level density reveals essentially two explanations for this surprising effect: the temperature-induced deformation due to the collective enhancement in the nuclear level density and the mutual support of magicities due to residual neutron–proton interactions which depend on the occupation of the single-particle levels.

In contrast to lighter systems, the evaporation residues of the most massive symmetric systems revealed some indication that the fusion and de-excitation processes are not decoupled by the intermediate stage of a compound nucleus but that they overlap in time and influence each other.

With the results of the investigations of the nearly mass-symmetric systems in mind, several characteristics found in the synthesis of the heaviest elements are analysed.

This review was received in March 1991.

0034-4885/91/070949+55$14.00

Contents

1. Introduction

The discovery of new elements was and still is a prestigious object of chemical research. Their synthesis, however, is only possible by means of nuclear reactions. Therefore, nuclear physicists joined the efforts of the chemists. The physicists were more generally interested to reach previously unexplored regions on the chart of nuclides, the coordinates of which are the number of protons and neutrons in the nucleus. They were particularly eager to extend the knowledge on the heaviest nuclei as an island of stability was predicted near the magic neutron number $N = 184$ and the proton number $Z = 126$ or 114 (Myers and Swiatecki 1966, Meldner 1967, Nilsson *et al* 1969, Mosel and Greiner 1969, Fiset and Nix 1972, Patyk and Sobiczewski 1990). As a prerequisite it was necessary to develop new experimental methods and to explore the characteristics of the possible production mechanisms.

The synthesis of new nuclear species relies on the constituents of the premordial nuclei available in nature. The available nuclei are limited in their neutron-to-proton ratio by the beta decay and in size by charged-particle decay and fission due to the increasing electrostatic repulsion between the constituent protons. The first method used to produce transuranium elements, which is still used to synthesize larger quantities of specific isotopes of elements from neptunium to einsteinium, was the consecutive capture of neutrons by uranium isotopes and the subsequent β^- decay of the capture products in nuclear reactors or in nuclear explosions. However, the number of nuclei attainable by this method is very limited.

A much more flexible method to aim directly at a specific heavy nucleus is the fusion of medium-heavy nuclei. In this case, the reaction products are inevitably rather excited. The excitation energy of the composite system gives rise to a de-excitation process in which the evaporation of particles competes with fission.

While a previous article in this journal (Münzenberg 1988) and other review articles (Armbruster 1985, Seaborg and Loveland 1985, Flerov and Ter-Akopian 1987, Seaborg and Loveland 1990) reported on the recent advances in the discovery of transuranium elements, the present work is intended to review the basic studies on the reaction aspects of the synthesis of heavy nuclei by fusion. In order to be able to control the conditions of the synthesis process, the dynamic evolution of the fusing system from the approach phase to the possible formation of a mononuclear system has to be understood. The subsequent de-excitation phase has to be investigated, especially the characteristics of the fission competition which tends to decompose the heavy nuclear system right after it has been formed. Some information on this subject may also be found in (Stokstad 1984, Armbruster 1987, Oganessian 1988).

The effects we expect to encounter in the synthesis of heavy nuclei may be illustrated by comparing this process with a simple classical example: the fusion of waterdrops. When two waterdrops are brought into contact they tend to reduce their total surface energy by forming one sphere. The excess energy may be removed by the evaporation of some molecules or by heat radiation. Although this classical model accounts well for the short-range nuclear force, nuclear dynamics show several important aspects which go beyond. First of all, nuclei cannot be understood without explicitly considering their quantum-mechanical properties which are responsible for

nuclear-structure effects. The long mean free path of the nucleons in the nucleus gives rise to a specific kind of dissipation, the one-body dissipation which is described by the wall-plus-window formula (Swiatecki 1980). Moreover, the repulsive Coulomb force decisively influences the fusion process as well as the de-excitation of heavy nuclear systems.

Understanding the fusion reaction is very much facilitated if we assume that the formation of the composite system and the de-excitation process are decoupled by the intermediate stage of a compound nucleus (Bohr 1936). That means that the de-excitation only begins when the excitation energy is distributed over all the degrees of freedom of the composite system. Thus, the only properties reminiscent of the entrance-channel phase are the excitation energy, the angular momentum, and the parity. While in the first sections we will assume that this hypothesis is fulfilled, we will finally check its justification and present some indications for a coupling between the entrance channel and the de-excitation process.

2. Experimental methods

Fusion cross sections have been determined by the observation of prompt x-rays (e.g. Karwowski *et al* 1982, Ernst *et al* 1982, Sujkowski *et al* 1983), delayed x-rays (e.g. Stokstad *et al* 1978, 1980a, b, 1989, Reisdorf *et al* 1982), γ rays (e.g. Almqvist *et al* 1960, 1964, Patterson *et al* 1971, Mazarakis and Stephens 1973, Cujec and Barnes 1976, Dayras *et al* 1976, Switkowski *et al* 1976, Wu *et al* 1978), and neutrons (e.g. Jahnke *et al* 1982) emitted from the fusion products.

If fusion products have to be observed directly, one may profit from their specific kinematic properties as they conserve the momentum of the projectiles in the laboratory frame. The evaporation of light particles broadens the velocity and angular distributions without changing the mean values. Therefore, the evaporation residues may be separated from the huge number of non-interacting projectiles, e.g. by a range selection or an in-flight ion-optical separation. While the first method allows the off-beam analysis of the radioactive reaction products accumulated in a catcher foil or in the gas of a helium jet, the second method requires an ion-optical device and makes it possible to apply in-beam identification methods.

Fusion products, once collected in a catcher medium, can be selected and identified by chemical methods, a review on which is given in the book of Seaborg and Loveland (1990). They also report on the use of mechanical separation tools like helium jet, drums, tapes, and wheels which are used to stop and to mechanically transport the reaction products to some radiation detector.

In-flight separation of the fusion products may be performed with any kind of magnetic or electric spectrometer, and many of those have been used for this purpose. Let us only mention the MIT–BNL velocity selector (Salomaa and Enge 1977), the velocity filter SHIP (separator of heavy ion reaction products) at GSI Darmstadt (Münzenberg *et al* 1979), the gas-filled magnetic separator SASSY (small-angle separatory system) at the Lawrence Berkeley Laboratory (Leino *et al* 1981, Ghiorso *et al* 1988), the electrostatic deflector at Argonne National Laboratory (Freeman *et al* 1983), the Munich recoil spectrometer (Rudolph *et al* 1983), the electrostatic deflector in Legnaro (Beghini *et al* 1985), and the electrostatic separator VASSILISSA at the Dubna Joint Institute for Nuclear Research (Yeremin *et al* 1989).

Three rather different experimental methods have proved to be the most successful for the observation of the heaviest nuclei. The helium-jet technique (Macfarlane and

Griffioen 1963, Bemis 1974) has been used at the LBL, a rotating-drum system (Oganessian *et al* 1975) has been applied for the observation of spontaneous-fission events in Dubna while the velocity filter SHIP (Münzenberg *et al* 1979) has been used for the experiments at GSI.

The velocity filter SHIP at GSI Darmstadt in combination with the heavy-ion accelerator UNILAC was also used to perform the experiments on the fusion studies of the most massive symmetric systems we will discuss later. As demonstrated schematically in figure 1, the velocity filter has two identical sections, each consisting of a quadrupole triplet for focusing and a sequence of two magnetic dipoles and one electric dipole working in a similar way to a Wien filter. More specific ion-optical information about SHIP may be found in Münzenberg *et al* (1979).

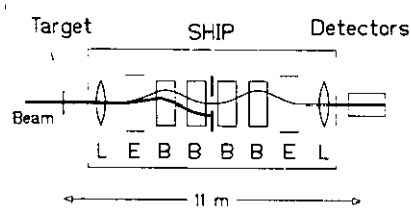

Figure 1. The ion-optical elements of SHIP. L: magnetic lens, consisting of three quadrupoles, E: electric dipole, B: magnetic dipole. The slit in the centre of the instrument defines the velocity range to be transmitted.

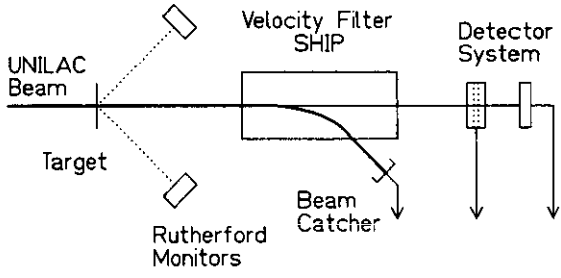

Figure 2. The most frequently used detectors for the experiments on heavy-ion fusion at SHIP.

The most important detectors used in fusion studies at SHIP are illustrated in figure 2. Elastically scattered projectiles and the electric current of the beam catcher are measured for normalization purposes. At the exit of the filter, time of flight and kinetic energy which are registered in a transmission start detector in combination with a silicon stop detector yield a rough mass determination of the nuclei which pass the separator. As the evaporation residues are implanted in the stop detector, it also serves for registrating their radioactive α decay or their spontaneous fission. Detection of these radioactive decays is the most sensitive tool for the identification of evaporation residues. In order to obtain additional information on the de-excitation process and on the radioactive decay of the fusion products, x-rays, γ radiation and charged particles may be registered in additional detectors around the target and around the stop detector.

The typical fingerprints of evaporation residues registered by time of flight and energy as well as by their radioactive α decay are presented in figures 3 and 4 for

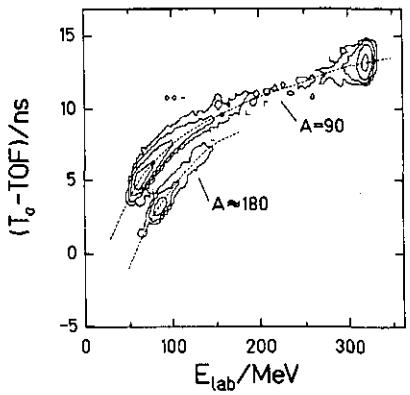

Figure 3. Two-dimensional spectrum of the time of flight and energy as registered behind SHIP in the reaction $^{90}Zr + ^{90}Zr$ at $E = 175.6$ MeV. The fusion products ($A \approx 180$) are clearly separated from the scattered projectiles ($A = 90$). From Keller (1985).

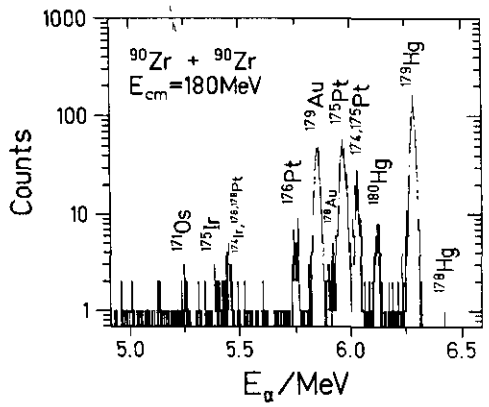

Figure 4. Spectrum of the radioactive alpha decay of the evaporation residues which are implanted in the stop detector behind SHIP in the reaction $^{90}Zr + ^{90}Zr$ at $E = 180$ MeV. The line at 6.12 MeV corresponds to the radiative-fusion product ^{180}Hg. From Keller *et al* (1986).

a specific reaction. The time sequence of the radioactive decays with respect to the implantation represents another important source of information for the identification of the evaporation residues. Ghiorso *et al* (1974) used the correlation to the subsequent α decay of the daughter nucleus to prove the synthesis of element 106. A comprehensive study of the statistical analysis of correlated events was formulated by Schmidt *et al* (1984b) and applied to establish the significance of the radioactive decay chains following the synthesis of the elements 107 to 109 (Münzenberg *et al* 1981, 1984a, b). In these cases, the method was further improved by correlating the position of the implantation and the subsequent decays by means of a position-sensitive stop detector (Hofmann *et al* 1984).

By the fusion of massive nuclear systems, very fissile compound nuclei may be produced. In this case, the bulk part of the fusion cross section leads to fission. For such systems, extensive investigations of binary reactions have been made (e.g. Lebrun *et al* 1979, Sahm *et al* 1980, Bock *et al* 1982, Tõke *et al* 1985, Shen *et al* 1987,

Back 1985, Back *et al* 1985, Keller *et al* 1987, Rivet *et al* 1988) by measuring the masses, energies and angles of the binary products in particle detectors around the target. It turned out that the compound-nucleus fission cannot always be distinguished unambiguously from other binary reactions, especially from deep-inelastic reactions and fast fission because their mass distributions overlap strongly (El Masri *et al* 1990), in contrast to evaporation residues which must always be preceded by the formation of a compound nucleus. These experiments, however, gave valuable information on the characteristics of binary reactions which compete with the formation of evaporation residues during the different reaction stages.

3. Fusion of massive systems

In this section we will investigate the characteristics of fusion, the first reaction stage of the synthesis process. First, we will recall the decisive influence of several nuclear properties on the fusion process which has been studied most extensively for light and medium-heavy systems. The conditions for cold fusion, i.e. for the production of compound nuclei with low excitation energies, will be considered. With increasing charge of the reaction partners, the probability increases that the excited fusion products decay by fission, and the evaporation residues may only represent a tiny fraction of the fusion cross section. The signature of fusion in the evaporation-residue cross section will be discussed and demonstrated for reactions between different isotopes of zirconium. Finally, the fusion of the most massive mass-symmetric systems, slightly heavier than $^{90}Zr + {}^{90}Zr$ up to $^{110}Pd + {}^{110}Pd$, will be studied for which the repulsive Coulomb force builds up a hindrance to fusion.

3.1. A reminder of the present understanding of the near-barrier fusion of light and medium-heavy systems

In the last decade, the experimental knowledge on fusion reactions of light and medium-heavy systems has grown considerably. Although the fusion of these lighter systems does not explicitly represent the subject of the present article, let us mention some of the most prominent experimental studies in this field: the fusion of ^{16}O with samarium isotopes has been studied at the Weizmann Institute of Science (Stokstad *et al* 1978, 1980a); fusion of $^{32,36}S$ with isotopes of molybdenum, ruthenium, and palladium has been investigated in Munich (Pengo *et al* 1983); fusion of isotopes of silicon, sulphur and chlorine with isotopes of nickel has been measured in Legnaro (Stefanini *et al* 1986, Skorka *et al* 1987); at Argonne, Freeman *et al* (1983) looked for the fusion of $^{58,64}Ni$ with tin isotopes; at Stony Brook, Berkowitz *et al* (1983) investigated the fusion of sulphur isotopes with magnesium isotopes and aluminium; a variety of systems has been studied at the Brookhaven National Laboratory, namely ^{40}Ca + different calcium isotopes (Aljuwair *et al* 1984) and combinations of germanium and nickel isotopes (Beckerman *et al* 1980, 1981, 1982, 1983); Stokstad *et al* (1980b) and Reisdorf *et al* (1985a) looked for the fusion of ^{40}Ar on isotopes of samarium and tin while Reisdorf *et al* (1985b) investigated the fusion of krypton with isotopes of germanium, molybdenum and ruthenium at GSI Darmstadt; careful experimental studies on a number of different systems have been performed at the Hahn-Meitner Institute in Berlin (Jahnke *et al* 1982). Recent review articles (Beckerman 1985, 1988 Reisdorf 1986) extensively summarize the present state of experimental information in this field. In addition to the measured excitation functions, for a large variety

of projectile–target combinations some reliable information on spin distributions has also become available recently (e.g. Stokstad *et al* 1989, Halbert *et al* 1989, Kühn *et al* 1989, Gil *et al* 1990b and references cited therein).

Originally it was considered adequate to describe the fusion by the penetration of the one-dimensional potential barrier (e.g. Bass 1974). In this picture, the potential was considered as a function of only one parameter, the distance of the nuclei, whereas the shape of the reaction partners was assumed to be frozen. However, a substantial enhancement of measured sub-barrier-fusion cross sections was found not to be compatible with the calculated transmission coefficients of the one-dimensional potential barrier (Stokstad *et al* 1980b, Vaz *et al* 1981, Reisdorf *et al* 1982, Balentekin *et al* 1983, Inui and Koonin 1984, Beckerman 1985). The efforts then concentrated on an examination of effects which could influence the internuclear potential. The understanding of the sub-barrier-fusion enhancement was improved by including the influence of the orientation of statically-deformed reaction partners (Wong 1973), of dynamic shape variations (Krappe *et al* 1983, Aguiar *et al* 1987, 1988, 1989a, Royer *et al* 1990, Ramamurthy *et al* 1990) and of zero-point shape fluctuations (Esbensen 1981) on the height of the potential barrier. In a more general description which includes these mechanisms, the quantum-mechanical coupling between the elastic channel and any other degree of freedom of the fusing system was shown to cause a splitting of the fusion barrier into several components (Dasso *et al* 1983, Broglia *et al* 1983a). The main characteristics of the data could be explained by including the coupling to the inelastic excitations of the reaction partners, the most important being their first 2^+ and 3^- states (Broglia *et al* 1983b), but the influence of the transfer-reaction channel on fusion has also been considered (Broglia *et al* 1983b, Rehm *et al* 1985).

The spin distribution populated in fusion and the energy dependence of the sub-barrier fusion cross section are expected to be closely related. In order to show this, we will write the fusion cross section $\sigma_{\rm fus}$ as a sum of the fractions of the geometrical cross section which lead to fusion as expressed by the fusion probability $p(E,l)$. The fusion probability depends on the centre-of-mass energy E and the angular momentum l.

$$\sigma_{\rm fus} = \pi\lambda^2 \sum_l (2l+1)p(E,l) \qquad \text{with} \quad \lambda^2 = \frac{\hbar^2}{2\mu E} \tag{3.1}$$

where μ is the reduced mass of the system.

In most fusion models the angular-momentum dependence of p can approximately be reduced to an energy dependence by including the centrifugal energy $E_{\rm rot}$ at the potential barrier:

$$p(E,l) \approx p(E - E_{\rm rot}, l = 0). \tag{3.2}$$

with

$$E_{\rm rot} = \frac{l(l+1)}{2\mu R_{\rm f}^2}\hbar^2$$

where $R_{\rm f}$ is the distance of the centres of the reactions partners at the potential barrier.

As the fusion cross section is a weighted sum of the fusion probabilities, shifted by the rotation energy at the barrier, the following relation results from relations (3.1) and (3.2) (Sahm *et al* 1985):

$$p(E,l) = \frac{1}{\pi R_l^2}\left[(E - E_{\text{rot}})\frac{\mathrm{d}\sigma_{\text{fus}}(E)}{\mathrm{d}E}\bigg|_{E=E_{\text{rot}}} + \sigma_{\text{fus}}(E - E_{\text{rot}})\right] \tag{3.3}$$

That means that any fusion model which fulfils relation (3.2) and which predicts the same fusion excitation function will yield the same spin distribution. Deviations from relation (3.2) which are expected due to variations of the shape and the position of the potential barrier with increasing angular momentum are discussed in Rowley *et al* (1989).

Recent experimental data (e.g. Gil *et al* 1985, 1990a, b, Kühn *et al* 1989, Stokstad *et al* 1989) nicely support the described close relation between the energy dependence of the cross section and the spin distribution in fusion. A more gradual slope of the fusion excitation function is reflected by a broader spin distribution. Other data show even somewhat higher angular momenta than expected from the fusion excitation functions (Vandenbosch *et al* 1986, Halbert *et al* 1989).

The most salient features found in the fusion of light and medium-heavy systems are the enhanced sub-barrier fusion and the broadening of the spin distribution around the barrier which seem to be closely related. The main characteristics of both can be explained by introducing the coupling to inelastic excitations and to the transfer-reaction channel (Landowne and Dasso 1984, Dasso *et al* 1989). However, the success of this model in simultaneously reproducing the measured excitation functions and the spin distributions, cannot be interpreted as a direct proof for this specific fusion model because relation (3.2) might also be fulfilled by other models. As pointed out by Mohanty *et al* (1990), the available data are equally well reproduced by assuming a single potential barrier which depends in height on the energy $E - E_{\text{rot}}$.

The present understanding of the fusion of light and medium-heavy systems as recalled in this section may serve as a basis for the interpretation of experimental data for more massive systems against which new effects will stand out.

3.2. Cold fusion

In synthesizing heavy nuclei, one is particularly interested in producing the composite system with low excitation energy in order to reduce the number of evaporated particles and thus to reduce the fission competition (Oganessian 1974). We now want to investigate the conditions under which this can be achieved, based on the behaviour of light and medium-heavy systems as described above.

The long-range electrostatic repulsion and the short-range nuclear forces between two nuclei form a potential barrier which has to be passed for fusion to take place. For a rough estimate one might assume that the reaction partners stay in their ground-state configuration up to the top of the barrier. While the electrostatic potential can be calculated easily, there exist several descriptions for the nuclear potential, e.g. an empirical description by Bass (1980), the proximity potential (Błocki *et al* 1977), the Yukawa-plus-exponential approach (Krappe *et al* 1979), and Hartree–Fock calculations (Berdichevsky and Reisdorf 1987). For illustration, figure 5 shows the electrostatic and the proximity potential between two ^{90}Zr nuclei. The repulsion predicted by the proximity description for small distances is an artefact, caused by the frozen-density approximation which does not allow for any deformation of the reaction

partners and leads to very high nuclear densities in the overlap zone. In reality the system will attain an energetically more favourable configuration by developing a neck.

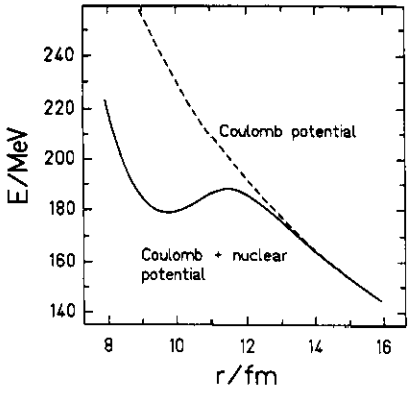

Figure 5. Calculated one-dimensional potential between two ^{90}Zr nuclei as a function of the distance of the centres. Broken curve: Coulomb potential. Full curve: sum of Coulomb and nuclear potential as given by the proximity descriptions of Błocki *et al* (1977).

If we take the height of this one-dimensional potential barrier as an approximate low-energy limit of fusion, the minimum excitation energy attained by fusion can be estimated by the following relation:

$$E^*_{\min} = B_{\text{pot}} + Q = B_{\text{pot}} + (m_{\text{p}} + m_{\text{t}} - m_{\text{CN}})c^2 \tag{3.4}$$

from the potential barrier B_{pot} and the Q value of the reaction which is given by the masses m of the compound nucleus (CN), the projectile (p) and the target nucleus (t). This quantity is shown in figure 6 for mass-symmetric systems.

The potential barrier, if calculated from one of the global nuclear potentials mentioned above, is a macroscopic quantity, i.e. it varies smoothly as a function of mass number A and charge Z of the reaction partners. The three masses involved in the Q value, however, include microscopical effects, that is, they fluctuate on a short-range scale in A and Z due to pairing correlations and shell effects. In figure 6 we also show the height of the fission barrier B_{fis} of the compound nucleus, which is important for the stabilization of the composite system. The quantities $E^*_{\min}$ and B_{fis} are directly comparable because both quantities refer to the ground state of the compound nucleus. In contrast to the one-dimensional fusion barrier which is considered under the condition of a frozen shape, the fission barrier is the lowest potential barrier which prevents the spherical compound nucleus from fission, whereby no condition on the shape is imposed. Consequently, the quantity $E^*_{\min}$ is always larger than the fission barrier (Mignen *et al* 1988). Both quantities, however, show some similarities in their general behaviour as a function of A and Z of the reacting nuclei when short-range fluctuations due to microscopic effects are neglected. For the heavy systems of interest here, $E^*_{\min}$ shows a minimum for mass-symmetric systems if the compound nucleus is fixed, shell effects in the Q value being neglected. This is in accordance with the fission barrier which, shell effects being neglected, is found to be lowest for symmetric mass splits for heavy systems (Businaro and Gallone 1957,

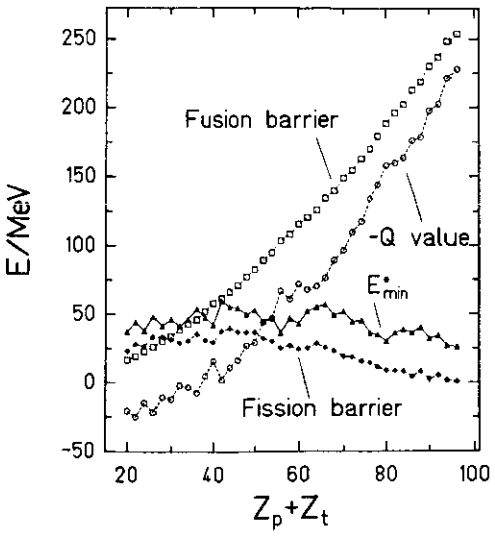

Figure 6. Comparison of the fusion barriers of mass-symmetric systems and the fission barriers of the corresponding compound nuclei as a function of the charge of the composite system. The sum of the fusion barrier and the Q value gives an estimate of the lowest excitation energy E^*_{min} of the compound nucleus to be reached by fusion. For every system, the mostly bound isotope was chosen as projectile and target. The fusion barriers were calculated with the proximity potential. The fission barriers were estimated from the liquid-drop barriers of Sierk (1986) with the ground-state shell effects subtracted. The ground-state shell effects are calculated as the difference of the experimental masses (Wapstra *et al* 1988) or semi-empirical mass values (Liran and Zeldes 1976) and the liquid-drop predictions of Möller and Nix (1981b). The Q values were calculated from experimental (Wapstra *et al* 1988) or semi-empirical mass values (Liran and Zeldes 1976).

Davies and Sierk 1985). Moreover, when symmetry is fixed, figure 6 demonstrates that both quantities, E^*_{min} and B_{fis}, decrease on the average with increasing charge for heavy compound systems. Very heavy systems are less stable against fission, but at the same time they can be produced rather cold. On a short-range scale, E^*_{min} is reduced if the reaction partners are especially well bound, and it is increased if the compound nucleus is strongly bound.

In accordance with the considerations of Oganessian (1974) we conclude that a specific heavy compound nucleus can be produced rather cold by a symmetric target–projectile combination due to the interplay of the potential barrier and the Q value; in addition, magic reaction partners are especially favourable.

The fusion of two ^{90}Zr nuclei forming ^{180}Hg is an interesting case which has been investigated in detail. The 50-neutron shell and the 40-proton subshell of projectile and target favour a cold fusion reaction, while the fission barrier of ^{180}Hg is high enough to ensure that the fission competition is not dominant in the de-excitation cascade for low angular momenta. The evaporation residues after the fusion of two ^{90}Zr nuclei as identified by their ground-state α decay (see figure 4) revealed a new type of reaction between heavy ions, the radiative fusion, that means the de-excitation of the composite system only by γ radiation without any loss of nucleons (Keller *et al* 1983). The excitation functions of the different evaporation channels show that the radiative fusion fits the regular dependence of the number of evaporated particles on the excitation energy, thus indicating that radiative fusion occurs as a statistical decay

channel which is favoured by the low excitation energy reached in this system. With the systematic considerations presented in figure 6, it can be understood that radiative fusion is likely to occur for very light and for very heavy systems only. Indeed, it was detected first for the light system $^{7}Li + {}^{16}O$ (Feldman and Heikkinen 1969). For light systems, the term radiative capture was used because these systems are captured in specific states of the compound nucleus. A review on radiative-capture reactions of light heavy ions is given by Sandorfi (1984). In the meantime, radiative fusion has been observed for a few other heavy systems: $^{90}Zr + {}^{89}Y$, ^{92}Zr, ^{94}Mo (Keller *et al* 1986), $^{50}Ti + {}^{208}Pb$ (Oganessian *et al* 1984).

3.3. How to extract the characteristics of fusion for compound systems with a strong fission probability

The observation of evaporation residues is an unquestionable indication for fusion; however, if fission is an important decay channel of the compound nucleus, evaporation residues only represent a fraction of the fusion cross section. One could think of deducing the experimental information on fusion from the study of binary reactions. But as we already mentioned, the distinction of compound-nucleus fission from other possible reaction channels is rather difficult because the signatures in the distributions of mass, energy and angle are not very clear, especially in mass-symmetric reactions. Thus, we prefer to deduce the fusion characteristics from measured evaporation-residue cross sections by estimating the partition of the fusion cross section in the different decay channels by a statistical-model calculation. It is clear that the deduced fusion characteristics depends on a reliable description of the statistical de-excitation process. Therefore, the parameters of the statistical model have to be chosen carefully. The cross section σ_{er} of evaporation residues can be described as the result of a two-step process:

$$\sigma_{er} = \frac{\pi\hbar^2}{2\mu E} \sum_{l} (2l+1)\, p(E,l)\, w(E+Q,l). \tag{3.5}$$

For every partial wave of angular momentum l, p describes the fraction of the geometrical cross section leading to fusion and w the probability of this part to survive the de-excitation phase against fission. The fusion probability is characteristic for the projectile–target combination, and it is a function of the centre-of-mass energy E and the angular momentum l. The survival probability is characteristic for the compound nucleus, and it is a function of its excitation energy $E^* = E + Q$ and its angular momentum l. Equation (3.5) is valid for the sum of all evaporation residues or for a specific subgroup, e.g. the evaporation of neutrons only, if σ_{er} and $w(E+Q,l)$ correspond to each other.

For the most heavy symmetric systems, the survival probability w, calculated with the statistical model, decreases faster with increasing l than the fusion probability p, deduced from measured excitation functions with relation (3.3). That means that the observation of evaporation residues yields an angular-momentum-weighted fusion probability, mostly representative for central collisions (Schmidt *et al* 1980, Sahm *et al* 1984, Reisdorf *et al* 1985b). The measured cross sections are even insensitive to the fusion probability at high angular momenta. In a model analysis, the fusion probability for $l = 0$ can be determined by fitting the measured evaporation-residue excitation functions with a fusion calculation followed by a statistical-model code.

The function $p(E,l=0)$ is chosen in a way to yield the best fit to the data. The angular-momentum dependence of the fusion probability is fixed by relation (3.2) or a similar description. Due to the limited experimental knowledge, usually there is some freedom to vary slightly some parameters, e.g. the fission barriers, in the evaporation calculation. These uncertainties of the evaporation calculation result in uncertainties of the extracted fusion probabilities.

If the same compound nucleus is formed with different projectile–target combinations, relative values of the fusion probability can be deduced by a direct comparison of the measured evaporation-residue cross sections. In addition, one might assume that rather mass-asymmetric systems with a low Coulomb repulsion in the entrance configuration fuse with the geometrical cross section at low angular momenta at energies somewhat above the barrier as is observed for light and medium-heavy systems (e.g. Gil *et al* 1985, Fischer *et al* 1986). With this assumption, even absolute fusion probabilities can be deduced which do not depend on the result of an evaporation calculation. However, for low excitation energies which are only reached in heavy mass-symmetric systems, the evaporation calculation is still needed in order to predict—or should we say extrapolate—the survival probability w to low excitation energies, which is needed for extracting the fusion probability p of the symmetric system. As structural effects in the level density are most important in this energy range they have to be incorporated very carefully in the analysis.

3.4. Systems at the threshold of hindrance to fusion

We will now consider the fusion of zirconium isotopes in more detail. The fusion of these systems behaves similarly to lighter systems, i.e. their fusion barrier is close to the predicted one-dimensional potential barrier, and they are characterized by an enhanced sub-barrier fusion. The measured excitation functions, however, are strongly influenced by the relatively high fission competition in the de-excitation of the compound nuclei. Slightly heavier systems which show a considerable deficit in the fusion cross section above the one-dimensional potential barrier are considered in section 3.5. In this sense, the systems presented here are situated at the threshold of hindrance to fusion.

First we will come back to the fusion of two ^{90}Zr nuclei since this system has been studied very carefully. The evaporation-residue cross section which was measured over many orders of magnitude (Beckerman *et al* 1984, Keller *et al* 1984) is shown in figure 7 as a function of energy.

The deduced fusion probability $p(E,l=0)$ of this system is also presented in figure 7. The survival probability $w(E^*,l)$ was calculated with the statistical-model code HIVAP (Reisdorf 1981). The parameters were fixed to their standard values as defined below in section 4.2. Only the empirical fission barriers of Dahlinger *et al* (1982) were slightly adjusted with a global scaling factor in order to comply with the assumption that the fusion probability p reaches unity in the saturation range well above the barrier. If compared with the calculated transmission across the one-dimensional potential barrier, the measured curve shows a somewhat smoother behaviour in the vicinity of the barrier, finally approaching the slope of the calculated curve well below the barrier. In the spirit of the coupled-channels approach discussed in section 3.1, the gradual increase of the fusion probability around the barrier is attributed to a splitting of the potential barrier. Keller *et al* (1986) deduced the experimental barrier distribution as shown in figure 7 by an unfolding procedure from the measured fusion-probability data by use of relation (3.8). This distribution can well be approximated

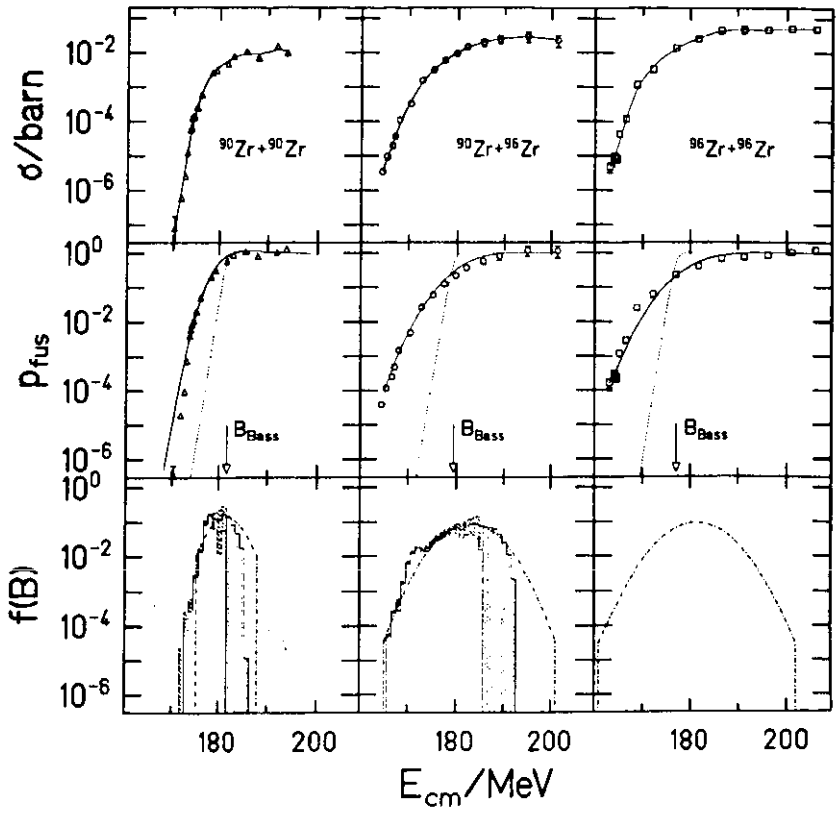

Figure 7. Measured excitation functions of evaporation residues (Keller *et al* 1986, Quint *et al* 1991), deduced fusion probabilities for central collisions and corresponding fusion-barrier distributions for the three systems indicated. For the systems ^{90}Zr + ^{90}Zr and ^{90}Zr + ^{96}Zr, the histograms in the lower part show the barrier distributions as obtained by an unfolding procedure (Keller *et al* 1986). The shaded areas indicate the uncertainty. The curves in the lower parts correspond to the fitted fusion-barrier distributions which were parametrized as truncated Gaussian functions. The curves to the measured excitation functions are drawn to guide the eye, those to the fusion probabilities are calculations using the fitted fusion-barrier distributions. The arrows indicate the potential barrier as calculated with the Bass potential (Bass 1980). The dotted curves correspond to the calculated transmission through the one-dimensional potential barrier B_{Bass}.

by a truncated Gaussian barrier distribution as demonstrated in figure 7. That way, one can express the experimental information on the barrier splitting by an analytical function. The fusion-barrier distribution $f(B')$ is characterized by three parameters, the mean value B, the standard deviation σ_B, and the truncation parameter t:

$$f(B') = n_0 \exp\left(-\frac{B - B'}{2\sigma_B^2}\right)^2 \tag{3.6}$$

for $|B - B'| < t\sigma_B$ and $f(B') = 0$ otherwise. The truncation parameter t determines the lowest barrier which may be realized by the coupling phenomena, the adiabatic

fusion barrier $B_{\text{adia}} = B - t\sigma_B$. The normalization n_0 ensures that

$$\int_{-\infty}^{\infty} f(B')\,\mathrm{d}B' = 1. \tag{3.7}$$

The fusion probability is given by a convolution of the barrier distribution $f(B')$ and the transmission coefficient $T(E - B', l)$:

$$p(E,l) = \int_{-\infty}^{\infty} f(B')\,T(E - B', l)\,\mathrm{d}B'. \tag{3.8}$$

The transmission coefficient may be calculated in the Wentzel–Kramers–Brillouin approximation (see e.g. Fröman and Fröman 1965, Will and Guinn 1988). For very heavy nuclei, the Hill-Wheeler approach (Hill and Wheeler 1953) which assumes the barrier shape to be an inverted parabola, with a curvature corresponding to a zero-point energy of $\frac{1}{2}\hbar\omega$, gives almost the same result:

$$T(E - B', l) = \{1 + \exp[-2\pi(E - B' - E_{\text{rot}})/(\hbar\omega)]\}^{-1} \tag{3.9}$$

where E_{rot} depends on the angular momentum l. For massive systems, $\hbar\omega$ amounts to about 4 MeV and varies also slightly with angular momentum. Below the adiabatic barrier, in the pure tunnelling regime, the fusion probability is almost parallel to the prediction of the one-dimensional fusion model.

Several systems in the vicinity of the threshold of hindrance to fusion have been investigated, namely ^{81}Br+^{90,94}Zr, ^{96}Mo, ^{104}Ru, (Beckerman *et al* 1984), ^{90}Zr+^{90,94}Zr (Beckerman *et al* 1982, 1984), ^{86}Kr + ^{92,100}Mo, ^{99,102,104}Ru (Reisdorf *et al* 1985b), ^{90}Zr + ^{89}Y, ^{90,92,96}Zr, ^{94}Mo (Keller *et al* 1984, 1986), and ^{96}Zr + ^{96}Zr (Quint *et al* 1991). We will concentrate on three systems in order to illustrate the influence of nuclear structure on the fusion process. In addition to the data of the system ^{90}Zr + ^{90}Zr, the corresponding experimental points and fitted parametrizations for the systems ^{90}Zr + ^{96}Zr and ^{96}Zr + ^{96}Zr are presented in figure 7. Obviously, the 6 valence neutrons in addition to the $N = 50$ shell broaden the barrier distribution deduced from the fit to the data very much. The contributions of the two reaction partners are not additive: the barrier distributions of the mixed and the neutron-rich system shown in figures 7 differ only little. A similar series of reactions between the nickel isotopes ^{58}Ni and ^{64}Ni (Beckerman *et al* 1982) has widely been discussed in the literature (e.g. Broglia *et al* 1983a, Landowne and Dasso 1984, Landowne and Pieper 1984). As in the nickel case, in the mixed system ^{90}Zr + ^{96}Zr the transfer-reaction channel may also strongly couple to the elastic channel and appreciably contribute to the width of the barrier distribution. The zirconium series is a test case for theoretical models, in which the overlap of the nuclear density distributions at the barrier is much larger than that in the nickel systems.

3.5. Evidence for hindrance to fusion of massive systems

Now we will proceed to study the fusion of more massive systems where new phenomena arise which have not been observed for lighter systems. The larger overlap of the nuclear density distributions at the potential barrier as well as the growing repulsive Coulomb force in the dynamic evolution of the system influence the fusion characteristics of these systems.

In a series of investigations, evaporation-residue cross sections have been measured for several heavy, nearly symmetric systems leading to compound nuclei up to thorium, and the apparent fusion-barrier shifts with respect to the one-dimensional potential barrier as well as the variance of the barrier distribution have been determined (Sahm *et al* 1985, Keller *et al* 1986, Quint *et al* 1991). For most of the data it was also necessary to introduce a truncation parameter which could be determined with good precision only in a few cases where the cross sections were measured at sufficiently low energies. The uncertainty of the truncation parameter has only little influence on the other two parameters of the fitted fusion-barrier distributions. The data are summarized in table 1.

Table 1. Paramaters of the fitted effective fusion-barrier distribution for massive nearly symmetric systems. Data are taken from: (a), Quint *et al* (1991); (b), Sahm *et al* (1985); and (c), Keller *et al* (1986). The mean barrier shift ($B-B_{\mathrm{Bass}}$) and the standard deviation (σ_B) were evaluated with two different evaporation calculations, using $E_d = 6$ MeV and $E_d = 18.5$ MeV, respectively. Those values for which the error bars are given correspond to the original publications. The others are added here in order to obtain a consistent set of data. The uncertainties account for the statistical errors only and are similar in both cases. For the Sn + Zr systems, the large damping constant was not used, because this would directly contradict the results obtained in the Ar + Hf series (see section 4.4). The cut-off parameter t was fixed to the indicated values in both cases. In this paper we will always refer to the data obtained with the small shell-damping constant $E_d = 6$ MeV.

		$E_d = 6$ MeV		$E_d = 18.5$ MeV			
System	B_{Bass}	$B - B_{\mathrm{Bass}}$	σ_B	$B - B_{\mathrm{Bass}}$	σ_B	t	
^{100}Mo + ^{110}Pd	209.9	21.1	8.3	29.0 ± 1.2	9.8 ± 0.4	4.0	(a)
^{100}Mo + ^{104}Ru	202.3	15.2	8.9	23.0 ± 1.1	10.2 ± 0.5	4.0	(a)
^{100}Mo + ^{100}Mo	193.8	7.8	5.7	12.2 ± 0.5	7.2 ± 0.2	4.0	(a)
^{100}Mo + ^{98}Mo	194.6	10.4	6.6	14.1 ± 1.0	7.6 ± 0.5	4.0	(a)
^{100}Mo + ^{96}Mo	195.4	10.4	6.5	10.4 ± 1.0	6.5 ± 0.4	4.0	(a)
^{100}Mo + ^{92}Mo	197.0	12.7	6.4	12.7 ± 2.2	6.4 ± 0.8	4.0	(a)
^{100}Mo + ^{96}Zr	185.4	9.5	7.0	9.5 ± 0.9	7.0 ± 0.4	4.0	(a)
^{100}Mo + ^{92}Zr	186.9	4.9	5.6	4.9 ± 1.0	5.6 ± 0.5	4.0	(a)
^{100}Mo + ^{90}Zr	187.6	5.1	6.2	5.1 ± 1.0	6.2 ± 0.4	4.0	(a)
^{86}Kr + ^{123}Sb	199.8	9.2 ± 0.4	4.2 ± 0.2	11.1	4.9	∞	(b)
^{86}Kr + ^{121}Sb	200.4	7.6 ± 0.5	4.9 ± 0.4	11.1	5.4	∞	(b)
^{124}Sn + ^{96}Zr	214.3	26.7 ± 0.5	8.9 ± 0.5			∞	(b)
^{124}Sn + ^{94}Zr	215.1	22.9 ± 0.7	8.8 ± 0.4			∞	(b)
^{124}Sn + ^{92}Zr	215.9	21.1 ± 3.0	7.8 ± 1.3			∞	(b)
^{124}Sn + ^{90}Zr	216.7	20.3 ± 3.0	6.9 ± 2.6			∞	(b)
^{90}Zr + ^{96}Zr	179.4	3.7	4.6	3.7 ± 0.3	4.6 ± 0.2	4.0	(c)
^{90}Zr + ^{92}Zr	180.9	3.7	4.2	3.7 ± 0.2	4.2 ± 0.1	3.2	(c)
^{90}Zr + ^{90}Zr	181.7	0.0	2.7	0.0 ± 0.2	2.7 ± 0.1	2.3	(c)

Whenever possible, the survival probability w in the de-excitation process of these systems was deduced from a comparison with measured evaporation-residue cross sections of several ^{40}Ar- and ^{48}Ca-induced fusion reactions leading to the same or at least to neighbouring compound nuclei (Vermeulen *et al* 1984, Sahm *et al* 1985). As the Coulomb repulsion is appreciably smaller than for the symmetric systems, it was assumed that the fusion of these asymmetric systems reaches the geometrical limit above the one-dimensional fusion barrier. For excitation energies which fall

below the fusion barriers of the asymmetric systems, the survival probabilities of the compound nuclei were extrapolated by an evaporation calculation using the code HIVAP (Reisdorf 1981). A major uncertainty stems from different assumptions on the behaviour of shell effects in the level density which manifest themselves mostly at low excitation energies. On the one hand, an analysis of neutron-resonance data and data on α-induced fission of nuclei around ^{208}Pb (Ignatyuk *et al* 1975, 1979) as well as microscopical calculations (Schmidt *et al* 1982) suggest that the shell effects damp out at about 20 MeV. On the other hand, systematic studies of different thorium isotopes across the 126-neutron shell (Vermeulen *et al* 1984, Sahm *et al* 1985) require a much stronger damping at around 6 MeV. A more detailed discussion on this subject follows in section 4.

In order to estimate an upper limit of the uncertainties introduced by different options of the statistical model, the fusion parameters deduced with two extreme assumptions are given in table 1 for most of the systems. On the one hand, a strong shell damping (E_d = 6 MeV) was used. On the other hand, it was assumed that the strong shell damping is a local phenomenon of thorium isotopes only, and the expected value of about 20 MeV was used for the analysis of the other systems. The largest difference appears in the barrier shift of the system ^{100}Mo + ^{110}Pd. In the following, we will restrict ourselves to the barrier-distribution parameters deduced with a strong shell damping (E_d = 6 MeV). However, we will ensure that the conclusions do not depend on the uncertainties due to the different analysis approaches.

Figure 8 presents the neutron-evaporation-residue cross sections, the fusion probabilities and the deduced effective fusion-barrier distributions of the systems ^{86}Kr + ^{123}Sb and ^{124}Sn + ^{96}Zr. When $Z_p \times Z_t$ varies from 1600 for ^{90}Zr + ^{90}Zr to 1836 and finally to 2000, the average fusion barrier increases suddenly if compared with the calculated one-dimensional potential barrier. If the proximity theorem (Błocki *et al* 1977) is valid, the nuclear potential of different nuclear systems is obtained from a universal proximity-potential function which only depends on the distance of the nuclear surfaces. This universal function is scaled by a factor which depends on the curvatures of the surfaces of the reaction partners. For three of the systems shown in figures 7 and 8, the half-density distance at the one-dimensional potential barrier, calculated with the proximity potential, varies from 1.52 fm for ^{90}Zr + ^{90}Zr to 1.49 fm for ^{86}Kr + ^{123}Sb and finally to 1.47 fm for ^{124}Sn + ^{96}Zr. In view of this small variation it seems to be impossible that the proximity-potential function can be modified in a way that the observed fusion barriers can be reproduced. Other effects than the one-dimensional potential must be responsible for the observed average fusion barriers. This was also concluded from studies based on Hartree–Fock calculations (Berdichevsky and Reisdorf 1987).

Let us first try to explain the data using the coupled-channels approach which was so successful for lighter systems. The barrier fluctuation is primarily represented by the width parameter σ_B. Here we prefer to use the asymptotic barrier shift D_∞ as a measure of the barrier fluctuation. D_∞ is defined as the displacement of the experimental fusion probability in the pure tunnelling regime with respect to the calculated transmission across the fitted mean barrier without fluctuations. This quantity is compared in figure 9 with the value of $D_\infty(2^+, 3^-)$ as expected from the coupling of the first 2^+ and 3^- levels of projectile and target to the fusion process (Reisdorf 1988). The simplified coupled-channels approach of Broglia *et al* (1983a) was used together with published values for the energies and the deformation lengths for the entrance-channel nuclei. This quantity, representing the collectivity

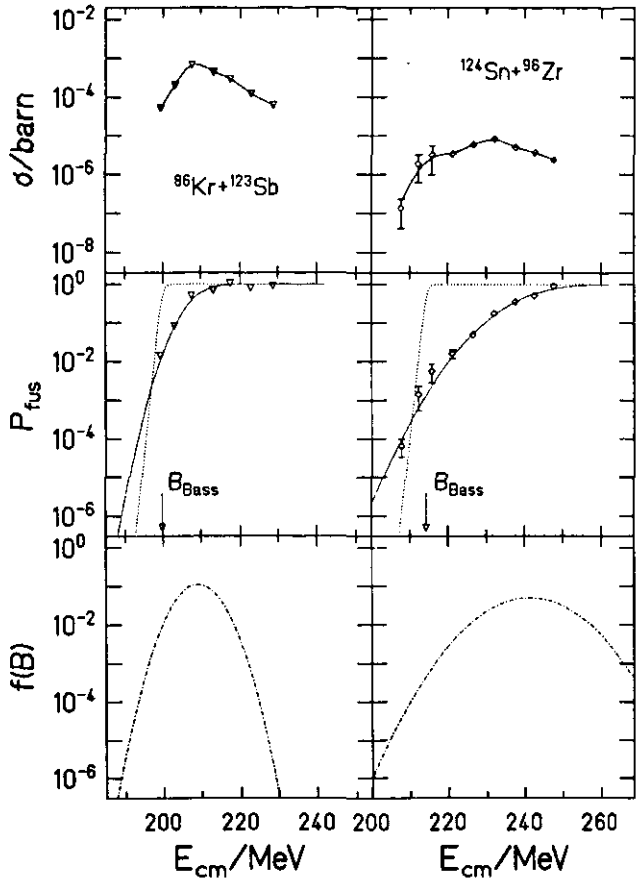

Figure 8. Measured excitation functions of evaporation residues, xn channels only (Sahm *et al* 1985), deduced fusion probabilities for central collisions and corresponding effective fusion-barrier distributions for the two systems indicated. For more explanation see figure 7.

and softness of low-lying states, which has proved to be successful in describing the characteristics of the fusion of lighter systems, is able to explain about half the observed effect. It is obviously also a good ordering parameter for the fluctuation phenomena in cases when the fusion is hindered. However, the coupling of the elastic channel to the low-lying states of the reaction partners is not able to explain the large shifts of the mean fusion barrier observed in these massive systems. Thus, one must conclude that, although the hindrance of fusion is strongly influenced by the same nuclear-structure properties as the sub-barrier fusion of lighter systems, new aspects must be considered in order to explain the huge mean barrier shifts. Depending on the nature of the processes involved, the picture of a distribution of potential barriers might be inappropriate and may be considered as an effective parametrization of the data only.

As one of the most salient features of the fusion-barrier distributions for the most massive systems listed in table 1, the diagram shown in figure 10 demonstrates that the occurrence of a large barrier shift is on the average correlated with a large variance of the barrier fluctuation. This behaviour is an indication that the fusion of these

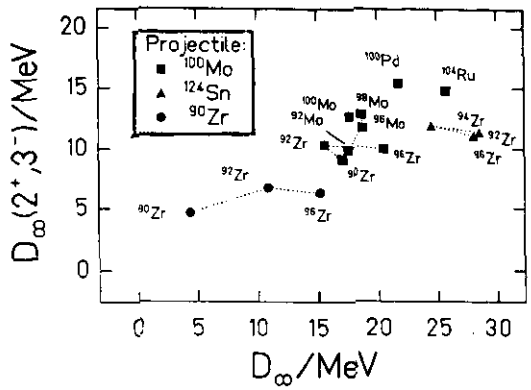

Figure 9. Correlation diagram of measured and calculated asymptotic barrier shifts. D_∞ is the shift between the steepest part of the measured excitation functions and a barrier-penetration calculation without fluctuations using the fitted mean barriers. The uncertainty is mostly given by the uncertainty of the fitted mean fusion barrier (see table 1). $D_\infty(2^+,3^-)$ is the calculated maximum barrier reduction due to coupling between the elastic channel and the first 2^+ and 3^- states of the reaction partners (Reisdorf 1988). The projectiles and the target nuclei are indicated.

systems is preceded by dissipative phenomena which introduce thermal fluctuations (Aguiar *et al* 1989b).

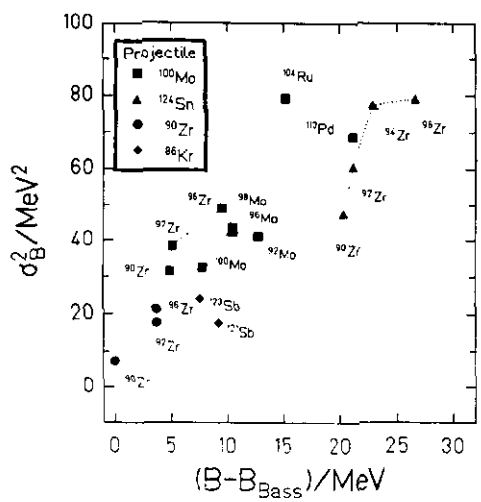

Figure 10. Two-dimensional plot, demonstrating the correlation between the mean shift $(B - B_{\mathrm{Bass}})$ and the variance σ_B^2 of the fitted effective fusion-barrier distribution. The uncertainties are given in table 1. The one-dimensional potential barrier B_{Bass} was calculated with the nuclear potential as given by Bass (1980). The projectiles and the target nuclei are indicated.

Essentially, there exist two macroscopic models which predict an appreciable hindrance to fusion. Gross *et al* (1981) as well as Fröbrich (1984) proposed strong surface-friction phenomena to occur when the system climbs up the potential barrier, resulting in a considerable loss of kinetic energy. Nix and Sierk (1977) as well as

Swiatecki (1981, 1982) pointed out that the passage of the one-dimensional potential barrier might not be sufficient for fusion to occur. By introducing a neck and a mass-asymmetry degree of freedom, they considered the further dynamic evolution of the system after being captured inside the one-dimensional potential barrier under the influence of the potential and inertial forces (Nix and Sierk 1977) as well as one-body dissipation (Swiatecki 1981, 1982). The 'extra-push' model of Swiatecki was developed further by different authors (Bjørnholm and Swiatecki 1982, Feldmeier 1982, Błocki *et al* 1986). For the almost mass-symmetric systems considered here, the mass asymmetry may be neglected. Figure 11 shows some dynamic calculations of Feldmeier (1982). After contact, the neck of the system grows rather quickly because this is connected with only little mass transport. Lighter systems fuse since they find themselves captured inside the fission barrier of the composite system while more massive systems develop towards immediate reseparation. Fusion may still be enforced by an additional kinetic energy, named extra push, in excess to the one-dimensional potential barrier. In the experimental data, this extra push manifests itself as a shift of the effective mean fusion barrier. In the above-mentioned formulations, both macroscopic models only predict the most probable reaction path. Fluctuation phenomena are not considered.

The ordering parameter for the extra-push model is Bass' entrance-channel parameter (Bass 1974, Swiatecki 1980) which is a measure for the ratio of Coulomb repulsion to nuclear attraction at half-density overlap:

$$x_e = \frac{4Z_pZ_t}{A_p^{1/3}A_t^{1/3}(A_p^{1/3}+A_t^{1/3})}((Z^2/A)_{crit})^{-1} \tag{3.10}$$

with $Z = Z_p + Z_t$ and $A = A_p + A_t$.

At this distance of the reaction partners the nuclear attraction in the proximity description is greatest. Consequently, there exists no fusion pocket for $x_e > 1$; that means the potential is repulsive everywhere and there is no driving force towards amalgamation. By use of the proximity potential one gets

$$(Z^2/A)_{crit} = 50.883(1 - 1.7826I^2) \tag{3.11}$$

with $I = (A - 2Z)/A$ being the neutron excess of the composite system.

For more mass-asymmetric systems, the evolution to mass symmetry which takes place in a rather compact configuration has to be considered in addition, and consequently the fusion hindrance is expected to be governed by a combination of the Bass parameter x_e and the fissility parameter $x_{fis} = (Z^2/A)/(Z^2/A)_{crit}$.

The predictions of the extra-push model were confirmed by experiments on the characteristics of binary events in reactions of different nuclei with ^{208}Pb (Bock *et al* 1982). However, these data are not directly comparable with the evaporation-residue data discussed above because they are sensitive to higher angular momenta. Moreover, the observed mass-symmetric binary events may include events without the formation of a compound nucleus.

In figure 12, the two macroscopic models are compared with the barrier shifts as deduced from the measured evaporation-residue cross sections of massive symmetric systems. According to numerical calculations of Błocki *et al* (1986), the barrier shift predicted by this version of the extra-push model scales with the parameter $x_{mean} = \frac{1}{3}x_{eq} + \frac{2}{3}x_{fis}$. Błocki *et al* assume that the neutron-to-proton ratio of the

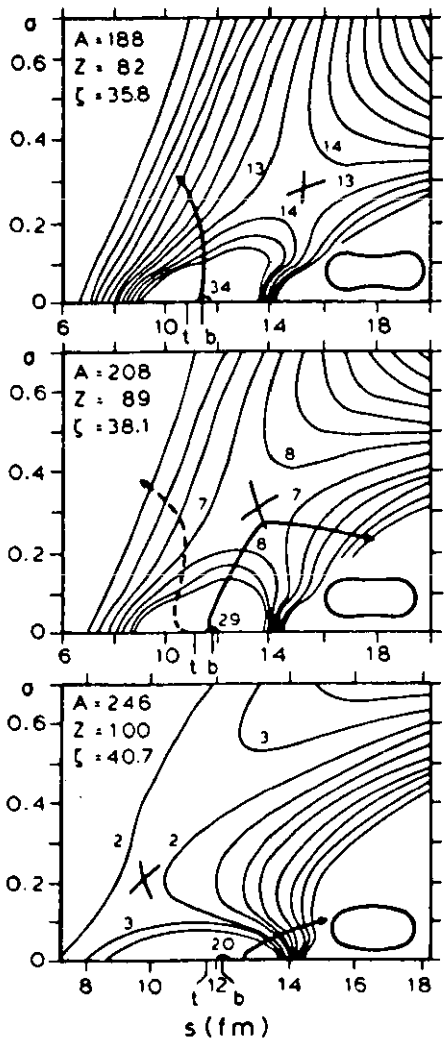

Figure 11. Calculated potential-energy landscapes for mass-symmetric systems as a function of the distance parameter s and the neck parameter σ (Feldmeier 1982). The mass number, the nuclear-charge number, and the effective fissility $\xi = Z^2/A$ of the compound nucleus are indicated. The numbers on the contour lines are the energies in MeV above the spherical compound nucleus. The fission-saddle point is indicated by the large cross. The saddle-point shape is shown in the lower right corner. The thick curve is a calculated head-on trajectory with an energy equal to the potential barrier. The broken curve is a trajectory starting at the touching point with no initial velocity. t: touching point. b: potential barrier. From Feldmeier (1982).

reaction partners equilibrates already at their very first contact. Therefore they use the parameter $x_{eq} = 4x_{fis}(\kappa^2 + \kappa + \kappa^{-1} + \kappa^{-2})^{-1}$ with $\kappa = A_p/A_t$. On the average, the experimental barrier shifts increase with the parameter x_{mean}. However, important deviations remain; in particular, the isotopic trends are found to be opposite to the predictions. If x_{mean} is the correct macroscopic ordering parameter, it seems that the influence of nuclear structure on the barrier shifts is strong enough to obscure a clear analysis of the underlying macroscopic trend.

The dissipation phenomena inherent in these macroscopic models are necessarily connected with fluctuations in the dynamic evolution of the nuclear system (Hofmann and Samhammer 1985, Canto 1989). Aguiar *et al* (1989b) and Fröbrich and Richert (1990) explicitly introduced fluctuation phenomena in the surface-friction model. Aguiar *et al* (1989b) came to the conclusion that this one-dimensional model is not able to describe the fusion of the most massive systems in a satisfactory way. In

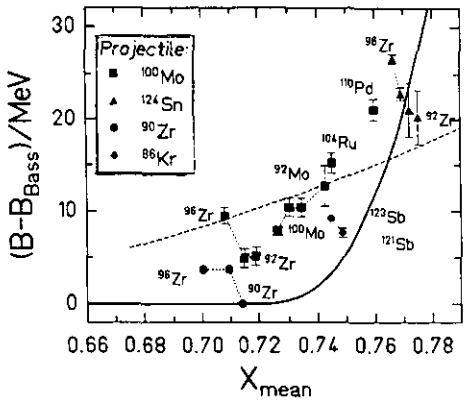

Figure 12. Fitted mean barrier shifts ($B - B_{Bass}$) as a function of the ordering parameter x_{mean} (see text). The experimental values (see table 1) are compared with the surface-friction model (broken curve) of Fröbrich (1984) and to the extra-push model (full curve) of Błocki *et al* (1986).

a recent work, Aguiar *et al* (1990) introduced thermal fluctuations in the extra-push model of Bjørnholm and Swiatecki (1982) and succeeded in reproducing the observed smooth increase of the fusion probability of the most massive systems quite well. But still the important nuclear-structure effects are not included.

Berdichevsky *et al* (1989) developed a model which predicts barrier shifts and fluctuations on a microscopic basis. It does not consider the later dynamic evolution of the dinuclear system simply assuming that fusion occurs in any case when the one-dimensional potential barrier is passed. In a two-centre shell-model calculation the energies of the different single-particle levels are determined as a function of distance up to the potential barrier. The initial occupation probabilities of these levels as determined by the pairing interaction are assumed to be preserved up to the barrier. This gives rise to an additional diabatic energy with respect to that of the energetically most favourable occupation distribution which determines the adiabatic potential. The initial occupation probability on partially-filled subshells of the reaction partners is subject to fluctuations which result in fluctuations of the diabatic potential. This extreme diabatic picture is justified by using results from the work of Bertsch (1978) by estimating that most nucleons stay in their initial orbits until the barrier is reached.

In figure 13, the predictions of the diabatic model are compared with the experimental results on apparent barrier distributions deduced from heavy-ion fusion reactions. There is a high degree of agreement in the structural behaviour of the barrier shifts and the widths of the barrier distributions. This underlines again that the fusion of massive nuclei is very much influenced by the nuclear structure of the reaction partners. The absolute values of the barrier shifts are somewhat underestimated for the tin-induced reactions which correspond to the largest values of the parameter x_{mean} (see figure 12). This might be a hint for an additional hindrance to fusion in the later dynamic evolution as predicted by the extra-push model.

The most massive symmetric system for which evaporation residues could be observed is $^{110}Pd + ^{110}Pd$ (Morawek 1991). Theoretical studies of the hindrance of fusion were made 17 years ago for this system (Sierk and Nix 1974). In this

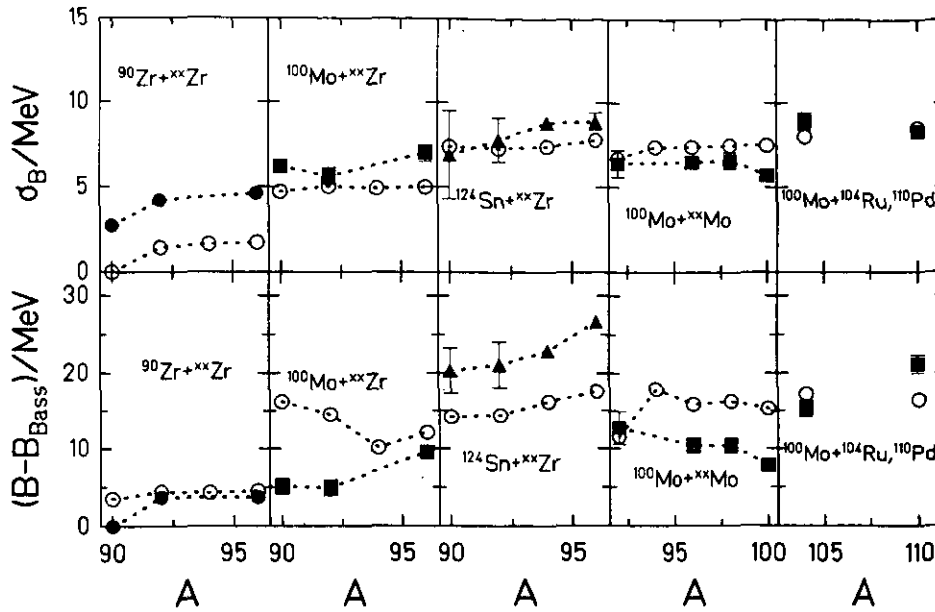

Figure 13. Survey of the predictions of the diabatic fusion model of Berdichevsky *et al* (1989). The measured (full points) as taken from table 1 and predicted (open points) mean barrier shifts $(B - B_{Bass})$ and standard deviations σ_B of the effective barrier distributions are compared for the systems indicated.

experiment, it could be proved that this system still fuses, in spite of the strong electrostatic repulsion in the entrance channel. However, in this case no attempt was made to deduce the fusion probability because of conceptional difficulties outlined in section 5. In figure 14, the energy-dependent evaporation-residue cross sections of three massive systems are compared: $^{100}Mo + ^{100}Mo$, $^{100}Mo + ^{110}Pd$ and $^{110}Pd + ^{110}Pd$. Some qualitative conclusions for the fusion of $^{110}Pd + ^{110}Pd$ may be drawn: the very gradual increase of the evaporation-residue cross section is the signature of a very broad effective fusion-barrier distribution. The low absolute cross sections are a combined effect of the hindrance to fusion and a strong fission competition in the de-excitation process. As the cross section increases over the whole range, it seems that the fusion does not reach the geometrical limit in the energy range investigated for central collisions.

In some other nearly symmetric systems which lead to even heavier composite systems, no evaporation residues could be observed (Gäggeler *et al* 1984). From these results, lower limits for the extra-push values have been deduced.

In conclusion we state that the fusion of massive nuclei is a very complex process. A complete theoretical description which traces the dynamical evolution of the system from the approach phase up to the possible capture inside the fission barrier of the compound nucleus with inclusion of microscopic effects and fluctuation phenomena is not yet available. For a comprehensive understanding of fusion, it seems to be necessary to understand the other reaction channels which compete with fusion during the different stages of the reaction, as well. The coupled-channels description makes clear that they all influence each other, and a specific reaction channel cannot be understood separately. This is why considerable effort is presently being made to improve the general knowledge on heavy-ion reactions by describing the fusion and

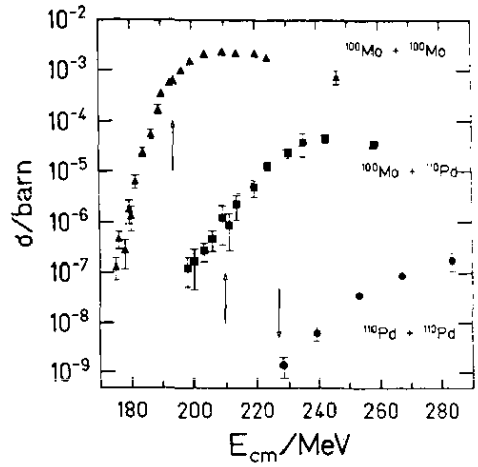

Figure 14. Measured evaporation-residue cross sections of the systems ^{100}Mo + ^{100}Mo, ^{100}Mo + ^{110}Pd and ^{110}Pd + ^{110}Pd (Morawek 1991). The calculated one-dimensional potential barriers (Bass 1980) are marked by the arrows.

the other competing reaction channels at the same time (e.g. Bellwied *et al* 1988).

4. De-excitation of heavy nuclei

While the fusion process is governed by nuclear dynamics, the de-excitation process is primarily determined by the statistical weight of the different de-excitation channels as treated by the statistical model (Bohr 1936, Bethe 1937, Bohr and Wheeler 1939, Weißkopf 1937, Blatt and Weißkopf 1952). The cold-fusion reaction is particularly well suited for comparing the predictions for the evaporation of particles and the emission of γ rays with experimental data because the evaporation cascade is short and thus the emitting system is rather well defined. As the fission competition plays a decisive role for the cross sections of heavy evaporation residues, this process will be extensively investigated, too.

4.1. Basic relations of the statistical model

The fusion process produces an excited nuclear system. In the present section we assume that this is a compound nucleus which is characterized by excitation energy, angular momentum and parity. Any other memory on the entrance channel is lost while the excitation energy is distributed over all degrees of freedom of the compound nucleus. In the de-excitation stage, several de-excitation modes—e.g. evaporation of neutrons, protons and light particles, emission of γ rays, and fission—compete with each other. This de-excitation phase, starting from the excited compound nucleus, is described by the statistical model. The decay probabilities $d^2P/(dt\,dE_f) = R$ per time and energy interval of the different de-excitation processes from a specific state, characterized by excitation energy E_i and spin J_i, into an energy interval between E_f and $E_f + dE_f$ and to a spin J_f are proportional to the product of the transmission coefficient T (or the strength function f in the case of γ rays) and the statistical weight ρ of the states to be reached. For the evaporation of the particle ν we have

to sum over all possible values and orientations of the angular momentum l and over all orientations of the intrinsic spin s of the evaporated particle:

$$R_\nu(E_i,J_i,E_f,J_f) = \frac{1}{\hbar}\frac{\rho(E_f,J_f)}{\rho(E_i,J_i)} \sum_{S=|J_f-s|}^{|J_f+s|} \sum_{l=|J_i-S|}^{|J_i+S|} T_l(\epsilon_\nu) \tag{4.1}$$

with $\epsilon_\nu = E_i - B_\nu - E_f$.

Mother and daughter nucleus are related by the kind of the evaporated particle ν. B_ν is the particle separation energy. The result for γ rays of multipolarity L is:

$$R^L_\gamma(E_i,J_i,E_f,J_f) = \frac{1}{\hbar}\frac{\rho(E_f,J_f)}{\rho(E_i,J_i)}\epsilon_\gamma^{2L+1} f_L(\epsilon_\gamma) \tag{4.2}$$

with $\epsilon_\gamma = E_i - E_f$.

The partial decay widths of the compound nucleus are given by:

$$\Gamma_\nu(E_i,J_i) = \hbar \int_0^{E_i-S_\nu} \sum_{J_f} R_\nu(E_i,J_i,E_f,J_f)\,\mathrm{d}\epsilon_\nu \tag{4.3}$$

$$\Gamma^L_\gamma(E_i,J_i) = \hbar \sum_{J_f=|J_i-L|}^{|J_i+L|} \int_0^{E_i} R^L_\gamma(E_i,J_i,E_f,J_f)\,\mathrm{d}\epsilon_\gamma \tag{4.4}$$

$$\Gamma_{\mathrm{fis}}(E_i,J_i) = \frac{1}{2\pi}\frac{1}{\rho(E_i,J_i)} \int_0^{E_i-B_{\mathrm{sad}}} \rho_{\mathrm{sad}}(E_i - B_{\mathrm{sad}} - \epsilon, J_i)\,\mathrm{d}\epsilon \tag{4.5}$$

B_{sad} is the height of the fission barrier, the rotational energy included. For calculating the fission width Γ_{fis}, the fission barrier is treated as a transition state defining the fission probability, irrespectively of the later development towards scission (Bohr and Wheeler 1939). We mention here that Swiatecki (1983) applied the transition-state method to derive a slightly different expression for the particle emission width Γ_ν.

Thus, the survival probability with respect to a specific channel ν can be expressed by:

$$w_\nu = \prod_n \left(\frac{\Gamma_\nu}{\sum_i \Gamma_i}\right)_n . \tag{4.6}$$

An evaporation calculation traces the compound nucleus over the different de-excitation steps n until a nucleus in its ground state is reached. In this way, it predicts the distribution of evaporation residues which are finally populated, as well as the probability of fission. In the presence of a high fission competition, the survival probability decreases nearly exponentially with excitation energy (see also Vandenbosch and Huizenga 1973).

The high degree of present understanding of compound-nuclear reactions is documented by Hodgson (1987). However, for a quantitative statistical-model calculation the nuclear binding energies, the fission barriers, and the level densities, as well as the transmission coefficients and the γ-strength function have to be known with sufficient accuracy. As the limited knowledge of these parameters is an essential source of uncertainty in the prediction of production cross sections in particular for heavy nuclei, it will be discussed in some detail in the following.

4.2. Expectations for the parameters of the statistical model

4.2.1. Binding energies. The binding energy has been measured for most of the known nuclei (Wapstra *et al* 1988). When measured values are not available, semi-empirical systematics or theoretical models (e.g. Haustein 1988) may be used for mass predictions. In the macroscopic–microscopic model (e.g. Möller and Nix 1988), the bulk (macroscopic) part of the nuclear binding energy is described by the liquid-drop model originally proposed by Weizsäcker (see Heisenberg 1932) and later improved by several authors (Myers and Swiatecki 1966, 1967, 1969, 1974, Myers 1977, Krappe *et al* 1979, Möller and Nix 1981a, Möller *et al* 1988). Shell-model calculations which are still less accurate on an absolute scale are used to determine the effects of shell and pairing corrections only. For this purpose, the binding energy is first evaluated from the single-particle level scheme, calculated in an appropriate nuclear potential well with residual interactions included (e.g. Rost 1968). The second calculation, performed with an averaged single-particle level scheme where shell effects are smeared out (Strutinsky 1967), serves to normalize this microscopic result to the macroscopic model description.

4.2.2. Nuclear level density. The nuclear level density may be calculated by use of the saddle-point method (Bohr and Mottelson 1975, Moretto 1972a) from the same single-particle level scheme as the ground-state shell correction. For a spherical nucleus the nuclear level density for one specific parity is given by

$$\rho(E,J) = \frac{\sqrt{a}(2J+1)\hbar^3}{48\sqrt{2\theta^3}U^2}\exp\left(2\sqrt{aU}\right) \tag{4.7}$$

where a is the level-density parameter which is related to the single-particle level density g at the Fermi surface ($a = g\pi^2/6$), U is an effective excitation energy above the yrast line, corrected for microscopic effects (see below), and θ the moment of inertia of the nucleus. The singularity of expression (4.7) at $U = 0$ may be removed by an iterative description of Grossjean and Feldmeier (1985).

The occupation probability of the single-particle levels around the Fermi surface varies more and more gradually when the nuclear temperature is increased. This is why the effects of shells and pairing correlations on the level density are expected to decrease and to finally vanish with increasing excitation energy (Bohr and Mottelson 1975, Huizenga and Moretto 1972). This temperature smearing of microscopic effects in the level density is equivalent (Bhaduri and Gupta 1973) to the computational smearing procedure (Strutinsky 1967) of the macroscopic–microscopic approach which is used to wash out microscopic effects in the nuclear binding energies. Hence, there is a close relation between the microscopic effects in the masses and in the level densities. Ignatyuk *et al* (1975, 1977) proposed an exponential function f for describing the washing out of the shell effects in the nuclear level density with increasing excitation energy, starting from the ground-state shell effects δU in the masses. The reduction of the energy-dependent pairing correlations in the level density may be expressed by multiplying a parabolic function h (Schmidt *et al* 1982) with the condensation energy δP.

$$U = E_{\text{eff}} + f(E_{\text{eff}})\delta U + h(E_{\text{eff}})\delta P \tag{4.8}$$

with

$$E_{\text{eff}} = E^* - \frac{l(l+1)}{2\theta}\hbar^2 + \begin{cases} 0 & \text{for even–even nuclei} \\ \Delta_0 & \text{for odd-mass nuclei} \\ 2\Delta_0 & \text{for odd–odd nuclei} \end{cases}$$

$$f(E_{\text{eff}}) = 1 - \exp(-E_{\text{eff}}/E_{\text{d}})$$

$$h(E_{\text{eff}}) = \begin{cases} 1 - (1 - E/E_{\text{c}}) & \text{for } E_{\text{eff}} < E_{\text{c}} \\ 1 & \text{for } E_{\text{eff}} \geqslant E_{\text{c}} \end{cases}$$

$\Delta_0 \approx 12/\sqrt{A}$, $\delta P = \frac{1}{4}g\Delta_0^2$ (Bohr and Mottelson 1975), and $E_{\text{c}} \approx 10$ MeV (Ignatyuk *et al* 1977). The variations of the quantities δU, δP and E_{c} with angular momentum may be deduced from microscopic calculations (e.g. Moretto 1972a, b).

From a systematic analysis of microscopic calculations, Schmidt *et al* (1982) corroborated the validity of this analytical description and determined the expected mass dependence of the shell-damping energy:

$$E_{\text{d}} = (0.4A^{4/3})/a \tag{4.9}$$

An illustration of the different dampings of even–odd structure and shell effects in the nuclear level density with increasing excitation energy is given in figures 15 and 16 with spectroscopic data of isotopes of Kr and Mo in the vicinity of the 50-neutron shell (Gaimard and Schmidt 1991). While the difference of the pairing condensation energy disappears already in the first few excited levels, the shell effect persists much further.

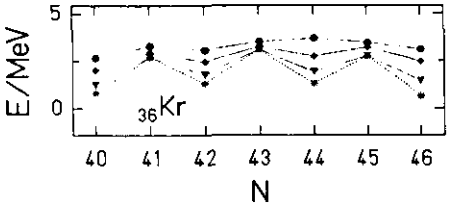

Figure 15. Pairing structure of krypton isotopes in the binding energies and in the level densities. Asterisks: Experimental microscopic corrections to the binding energies as given by the differences of the experimental masses (Wapstra *et al* 1988) and those of the liquid-drop model (Myers and Swiatecki 1966). The other symbols give the sum of these microscopic corrections and the measured excitation energies of the 2nd, the 21st and the 44th level with degeneracies taken into account. From Gaimard and Schmidt (1991).

Due to the close relation between microscopic effects in the binding energies and in the level density, an estimate of the level density might be obtained by introducing the 'experimental' shell effect as defined by the difference of the experimental binding energy and the prediction of the liquid-drop model in the analytic formulae given above. If experimental binding energies are available, this estimate might be more realistic than an independent microscopic calculation which does not reproduce the experimental shell effect precisely. In analogy with the macroscopic–microscopic model for the masses as presented above, the level densities may be described by

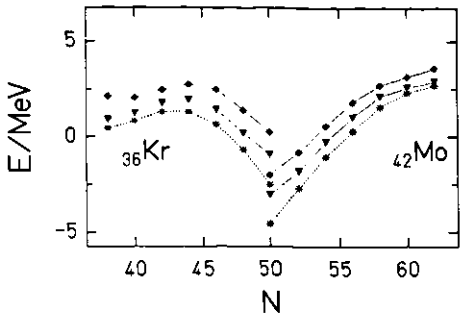

Figure 16. Shell structure of even–even krypton and molybdenum isotopes in the binding energies and in the level densities. Asterisks: see figure 15. The other symbols give the sum of the microscopic corrections and the measured excitation energies of the 2nd and the 21st level with degeneracies taken into account. From Gaimard and Schmidt (1991).

combining the analytical relations (4.7) to (4.9) with an analytical description of the macroscopic level-density parameter a for nuclei without shell effects and pairing correlations as developed by Töke and Swiatecki (1981).

$$a = \frac{A}{14.61\ \text{MeV}}(1 + 3.114A^{-1/3}F_2 + 5.626A^{-2/3}F_3) \tag{4.10}$$

The quantities F_2 and F_3 are the surface area and the integrated curvature of the surface, respectively, relative to the values for spherical shape (Myers and Swiatecki 1974).

The intrinsic nuclear level density described above completely represents the nuclear levels; the energies of specific levels, however, may be more or less affected by residual interactions which are neglected up to now. In particular, the collective motions which represent a combination of correlated single-particle excitations appear at comparatively low energies and tend to enhance the nuclear level density there. Nuclear spectroscopy reveals a considerable contribution of rotational and vibrational levels to the nuclear level density at low energies. This collective enhancement of the level density depends on the shape and the stiffness of the nucleus. Theoretical estimates have been made in order to predict the temperature dependence of the collective enhancement (Bjørnholm *et al* 1974, Hansen and Jensen 1983, Maino *et al* 1990). Ignatyuk *et al* (1979) extracted the temperature dependence from measured fission probabilities. From these studies one expects that the collective enhancement persists to rather high energies, of the order of 100 MeV. At first sight, it should have only little influence on the de-excitation process, because the collective bands are built up on each intrinsic level and no specific de-excitation process seems to be particularly favoured. An explicit formulation of the nuclear level density for deformed nuclei with and without collective contributions included can be found in (Ignatyuk *et al* 1979, Reisdorf *et al* 1985b).

4.2.3. Fission barriers. The measured fission-barrier parameters, mostly deduced from measured fission cross sections in light-particle-induced reactions, were compiled by Dahlinger *et al* (1982). From these data they deduced an empirical liquid-drop description:

$$B_{\text{fis}} = 0.7332\ 10^{u}\ Z^2/A^{1/3} \tag{4.11}$$

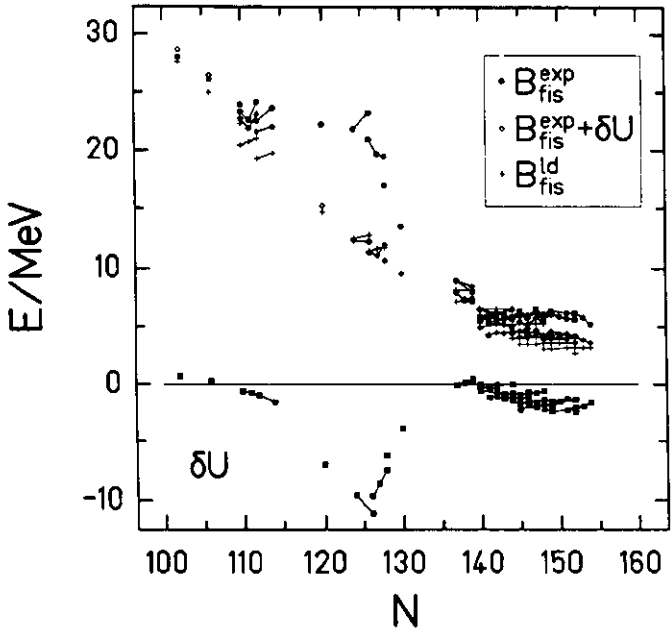

Figure 17. Lower part: experimental shell effects δU, calculated as the difference of the experimental masses (Wapstra *et al* 1988) and the liquid-drop masses (Möller and Nix 1981b). Upper part: The full points correspond to the measured fission barriers B_{fis}^{exp}. They clearly show the influence of the shell effects around ^{208}Pb. The open points which represent the sum $B_{fis}^{exp} + \delta U$ are close to the liquid-drop fission barriers (crosses) from Dahlinger *et al* (1982). (A similar figure was shown by Myers (1977).)

with $u = 0.368 - 5.057x_{fis} + 8.93x_{fis}^2 - 8.71x_{fis}^3$ and $x_{fis} = 49.22(1 - 0.3803I^2 - 20.489I^4)Z^2/A$ with $I = (N - Z)/A$.

The theoretical prediction of fission barriers relies on the determination of the saddle point in the calculated shape-dependent potential-energy surface. Sierk (1986) calculated the angular-momentum-dependent macroscopic fission barriers with a finite-range liquid-drop description. These values for angular momentum zero are close to the empirical description given above, except for a small difference in the isotopic trend. Finite-range effects which are not included in the above-given liquid-drop description are not important for the heavy nuclei considered here. The fission barrier is the sum of the liquid-drop barrier plus shell corrections in the ground state as well as at the barrier. For nuclei around ^{208}Pb, figure 17 demonstrates that a reasonable estimate of the fission barrier is obtained by only adding the gain of binding energy due to the shell effect in the ground state to the liquid-drop fission barrier. Shell effects at the saddle point do not seem to have a strong influence on the height of the fission barrier, although they are known to create a second minimum in the potential landscape, responsible for the existence of fission isomers. They have, however, a decisive influence on the shape of the nucleus at the fission barrier and thus on the contribution of rotational levels to the level density at low energies above the saddle point (Britt 1980). Special efforts have been made in order to empirically extract the isotopic trends of the liquid-drop fission barriers from the measured isotopic sequences, and indications for a reduction of the barriers near the proton drip line compared with other liquid-drop descriptions have been found (Dahlinger *et al* 1982).

4.2.4. Transmission coefficients. The transmission coefficients for the emission of particles from the excited compound nucleus are given by the quantum-mechanical penetration of the potential barrier (Alexander *et al* 1990). There exists a long-standing discussion on experimental charged-particle spectra which indicates apparent lower barriers than expected (Knox *et al* 1960, McMahan and Alexander 1980, Rivet *et al* 1982, Moses *et al* 1985, 1987, Nebbia *et al* 1986, La Rana *et al* 1987, Lacey *et al* 1987, 1988). From a comprehensive study, Vaz and Alexander (1984) concluded that the energy spectra of evaporated charged particles (protons and α particles) are described by lower potential barriers than the cross sections of fusion induced by the same particles. In special cases it was shown that at least part of these differences depends on the model analysis (Govil *et al* 1987, Gollerthan 1988). The deduced barrier reduction for evaporated charged particles is most pronounced for high excitation energies (100 MeV or higher) where the analysis is particularly difficult. One source of uncertainty for the analysis of the high angular momenta of the excited nuclei involved is the assumed shape of the Yrast line.

4.2.5. γ-strength function. The γ-strength function can be described in the independent-particle model (Blatt and Weißkopf 1952). Empirical values for the transition rates are exceptionally high for collective transitions (e.g. E2 transitions between the levels of a rotational band).

For higher transition energies the giant resonances are important. The electric dipole resonance gives the largest transition rates. The appropriate γ-strength function is described by the following Lorentzian function (see e.g. Snover 1986):

$$f_{E1} = 3.31 \times 10^{-6}\ \mathrm{MeV}^{-1} \frac{NZ}{A} \frac{\epsilon_\gamma \Gamma}{(E_0^2 - \epsilon_\gamma^2)^2 + \epsilon_\gamma^2 \Gamma^2} \tag{4.12}$$

if it exploits the Thomas–Reiche–Kuhn sum rule (see Levinger 1960).

For heavy nuclei, the resonance energy can be described by the droplet model (Myers *et al* 1977):

$$E_0 = 167.23 A^{-1/3}(1.959 + 14.074 A^{-1/3})^{-1/2}\ \mathrm{MeV}. \tag{4.13}$$

The width Γ is found to be about 5 MeV for all nuclei. As first proposed by Brink (1955), a giant dipole resonance (GDR) can be built up on each nuclear level, so that the GDR can decay also to excited levels of the compound nucleus. Similar descriptions exist for other giant resonances which are, however, less important for the statistical de-excitation process.

From the above, it seems that our knowledge of the parameters of the statistical model is already rather complete. It serves to establish a well defined basis for analysing measured data in order to pin down the origin of possible deviations. Some important ideas which go beyond the above description deal with induced deformations with increasing temperature by the statistical weight of rotational levels (Vigdor and Karwowsky 1982, Schmidt *et al* 1984a) and strong neutron–proton interactions (De Shalit and Goldhaber 1953, Schmidt and Vermeulen 1980, Zeldes *et al* 1983, Hamilton *et al* 1985) which are usually not accounted for in shell-model calculations. We will come back to these subjects in section 4.5.

4.3. Particle evaporation and gamma emission in a cold-fusion reaction

As the system $^{90}Zr + ^{90}Zr$ was found to be particularly well suited to reach low excitation energies, this system or close neighbours were chosen to perform comprehensive studies of the emission of charged particles and γ rays in the de-excitation process. Such investigations are very difficult for still heavier systems, because the increasing fission competition cuts down the cross section of evaporation residues appreciably.

Experiments on the systems $^{90}Zr + ^{89}Y$ and $^{90}Zr + ^{90}Zr$ were performed at the velocity filter SHIP. The experimental set-up as sketched in figure 2 was completed by a silicon detector telescope which covered forward angles and an assembly of NaI detectors which covered almost 4π around the target (see figure 18). The angular range of the forward telescope was limited by the condition that the residues after the evaporation of an α particle which was detected in the telescope fall well into the angular acceptance of SHIP.

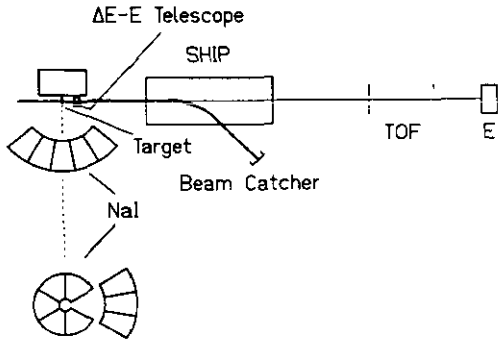

Figure 18. Schematic drawing of the experimental set-up for the investigation of γ radiation and charged-particle evaporation in coincidence with the identification of the evaporation residues behind SHIP (Schmidt *et al* 1986, Gollerthan *et al* 1991). Lower part: cut perpendicular to the beam at the target position showing the NaI detector assembly.

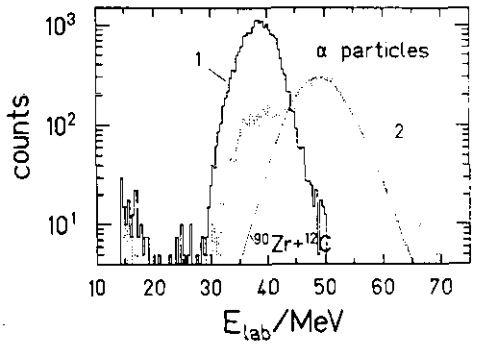

Figure 19. Energy spectra of alpha particles. 1: alpha particles registered in coincidence with an evaporation residue. 2: alpha particles registered without the requirement of this coincidence (measured in a shorter time). The spectrum marked $^{90}Zr + ^{12}C$ (dotted curve) represents an alpha spectrum calculated with the statistical-model code CODEX, assuming a fusion reaction between ^{90}Zr projectiles and ^{12}C target nuclei. From Gollerthan *et al* (1991).

Figure 19 demonstrates that this complex set-up is necessary in order to obtain clear experimental information. The charged-particle spectra registered without requiring the coincidence of an evaporation residue identified behind SHIP by the TOF-energy set-up are dominated by more abundant events emerging from reactions of the projectiles with light-element impurities in the target. Only the delayed coincidence with the arrival of an evaporation residue with $A \approx 180$ assures an undisturbed spectrum of charged-particles evaporated from the fusion products. By requiring the same delayed coincidence with evaporation residues behind SHIP, also background-free γ-ray spectra from the fusion products can be obtained.

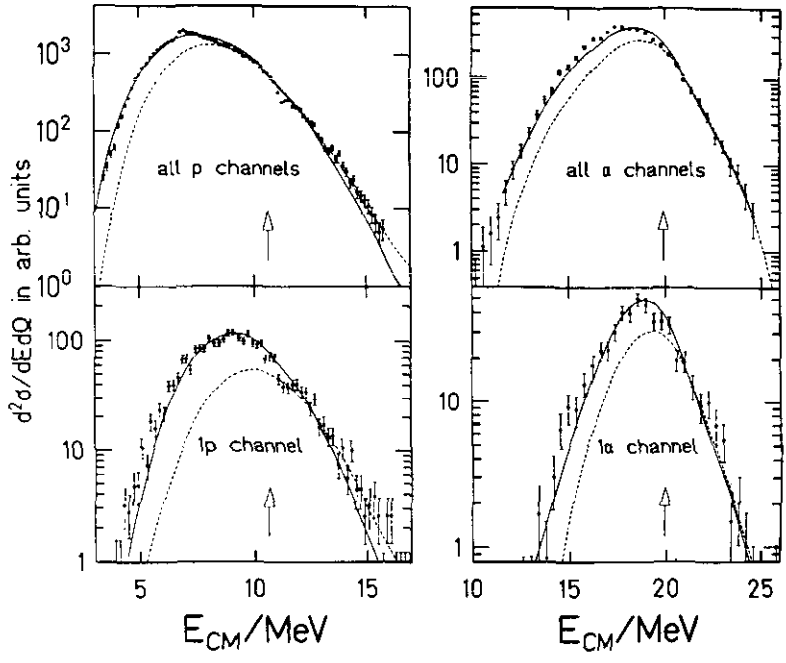

Figure 20. Spectra of protons (from all proton channels as well as from the 1p channel only) and α particles (from all α channels as well as from the 1α channel only) in the reaction $^{90}Zr + ^{89}Y$ at $E = 181$ MeV. Points: experimental data; broken curves: calculation assuming spherical nuclei; full curve: calculation with shifted transmission coefficients (−0.7 MeV for protons, −0.4 MeV for α particles); arrows: barriers as calculated for spherical nuclei. From Gollerthan *et al* (1991).

By imposing windows on the sum of the total γ energy and the registered proton- or α energy, four groups of evaporation channels can be distinguished at an excitation energy of 26 MeV (see figure 20). The complex information on charged-particle spectra for these different groups as well as the evaporation-residue cross sections can satisfactorily well be reproduced by an evaporation calculation with the Monte-Carlo code CODEX (Gollerthan *et al* 1991) by use of the above-described options (see section 4.2). The distribution of fusion barriers was adjusted to the data. A shift of −400 keV was applied to the transmission coefficients of the α particles in order to account effectively for the expected ground-state deformation ($\delta \approx 0.3$) of ^{179}Au. For reproducing the measured proton spectra, the corresponding transmission coefficients had to be shifted by -700 ± 330 keV with respect to the expectation of the fusion-

barrier systematics of Vaz and Alexander (1984) for spherical nuclei. This shift is much too large to be explained by the deformation of ^{179}Au. This discrepancy should not be stressed too much, because proton-induced fusion could only be studied with stable target nuclei, whereas the compound nucleus ^{179}Au is far away from the valley of β stability. Thus, the potential deduced e.g. from the measured fusion cross section in the reaction $^{1}H + ^{197}Au$ cannot be used directly but has to be scaled with the help of a model calculation, e.g. by use of the relations of the droplet model (Myers and Swiatecki 1974, Myers and Schmidt 1983) in order to predict the potential barrier for the evaporation of protons from the compound nucleus ^{179}Au.

Detailed γ-spectroscopic investigations were performed (Schmidt *et al* 1986) on the system $^{90}Zr + ^{90}Zr$ at $E = 179$ MeV which corresponds to an excitation energy of 21 MeV of the compound nucleus ^{180}Hg. The cross section for radiative fusion amounts to 40 μb. The γ rays were tagged by delayed coincidences with the radioactive ground-state decays of ^{180}Hg ($E_\alpha = 6.12$ MeV, $t_{1/2} = 2.9$ s) and ^{179}Hg ($E_\alpha = 6.29$ MeV, $t_{1/2} = 1.09$ s) in order to obtain separate information on the radiative-fusion and the 1n evaporation channel. It turned out that both γ spectra as shown in figure 21 as well as the measured cross sections of the radiative fusion and the 1n channel can be described by the statistical model when the γ strength of the electric giant dipole resonance is used. Clear information on the splitting of the resonance energies due to a possible deformation of ^{180}Hg and ^{179}Hg cannot be obtained because the γ spectra could not be measured at sufficiently high energies due to the lack of statistics.

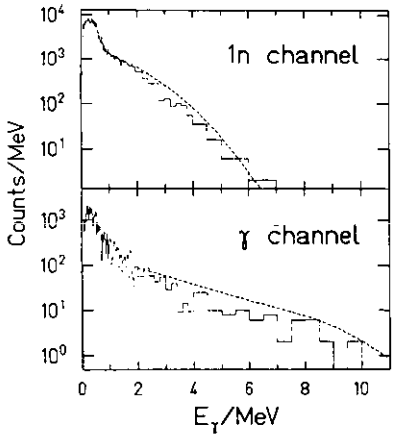

Figure 21. Histograms: γ spectra corresponding to the radiative fusion and the 1n channel measured in the reaction $^{90}Zr + ^{90}Zr$ at $E = 179$ MeV. Broken curves: statistical-model calculation with standard parameters using the electric giant dipole resonance. From Schmidt *et al* (1986).

These investigations showed that the de-excitation process after the fusion of the systems $^{90}Zr + ^{90}Zr$, ^{89}Y is well understood by the statistical model using standard parameters, except the previously mentioned slight reduction of the barrier for the evaporation of protons.

4.4. Fission competition in heavy-ion fusion reactions

It has been shown recently that the fission of an excited nucleus cannot be treated as a

purely statistical process, determined by the number of available doorway states above the fission barrier. As already formulated by Kramers (1940) and later stressed by Grangé and Weidenmüller (1980) and Grangé *et al* (1983), the dynamic evolution of the compound nucleus from the spherical or near-spherical ground-state shape to the saddle-point deformation is a dissipative process which may prevent the fission width from reaching the value predicted by the statistical model. This dissipative reduction of the fission width was incorporated in statistical-model codes (e.g. Delagrange *et al* 1986), and an enhanced particle evaporation was predicted. From experimental investigations of evaporated particles in coincidence with fission fragments (Hinde *et al* 1989) it may be concluded that the evaporation of particles before scission is enhanced with respect to the statistical-model prediction if the excitation energy of the compound nucleus exceeds approximately 50 MeV (see figure 22). If we take into account that a large portion of the particles is evaporated on the way from the saddle point to the scission configuration, i.e. after having passed the doorway states of fission, we expect that in the synthesis of heavy nuclei which is performed at the lowest possible energies the dissipative reduction of the fission competition only plays a minor role. Therefore, this effect will not be considered in this section, and instead we assume the statistical model to be applicable.

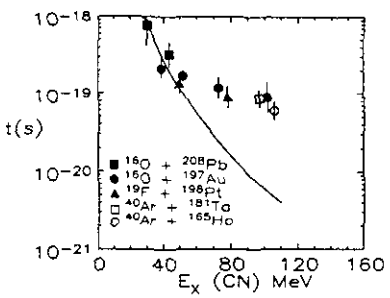

Figure 22. Minimum time required to emit the observed number of neutrons for fission following the indicated reactions, leading to fissile nuclei. The curve shows roughly the minimum time required to emit the neutron multiplicities as calculated with the statistical model (from Hinde *et al* 1989).

General considerations and a systematic survey of the fission competition in the de-excitation process of heavy nuclei can be found in Vandenbosch and Huizenga (1973). They attribute its magnitude primarily to the global trends in the fission barriers and in the neutron separation energies. In addition to the macroscopic trends, both quantities are strongly modulated by shell effects. It is of particular interest for the estimation of the attainable cross sections of nuclei near the not-yet-reached predicted doubly-magic nucleus $^{298}114$ to obtain a quantitative understanding of a possible stabilizing influence of the ground-state shell effect on the fission competition.

The half-life of spontaneous fission from the ground state is known to be strongly influenced by the magnitude of the shell effect in the ground-state binding energy (Swiatecki 1956, Patyk *et al* 1988). In this case, the decisive quantities for the penetration of the fission barrier are its height and its thickness. In the de-excitation process, the decisive quantities for the fission competition are the height of the fission barrier and the level density above the fission barrier of the initial nucleus as well as the level density above the ground state of the daughter nucleus after particle

evaporation. Thus, one also expects a considerable influence of the ground-state shell effect on the fission competition.

Fission cross sections in α-induced reactions were used to deduce fission barriers and energy-dependent level densities of nuclei in the vicinity of the doubly-magic nucleus ^{208}Pb (Moretto *et al* 1972, Ignatyuk *et al* 1980). For these only slightly-fissile nuclei, the fission cross section very sensitively reflects the fission competition in the de-excitation process while the formation of evaporation residues represents the dominant de-excitation channel and consequently exploits almost the whole cross section. For heavier, more fissile, nuclei the situation is reversed. When fission is the dominant de-excitation mode, the evaporation-residue cross section is very sensitively determined by the fission competition in the de-excitation process.

Highly-fissile nuclei with strong but well-localized shell effects are only available around $N = 126$ and $Z > 88$. For a systematic study, a series of thorium compound nuclei from ^{216}Th to ^{224}Th was produced in ^{40}Ar- and ^{48}Ca-induced reactions (Vermeulen *et al* 1984, Sahm *et al* 1985). In this way, residues on both sides of the $N = 126$ shell were produced by the evaporation of neutrons. The evaporation-residue cross sections (xn, pxn and αxn channels) were studied for altogether 8 reactions from below their respective fusion barriers up to about 30 MeV above. Figure 23 shows these for the system ^{40}Ar + ^{180}Hf as an example.

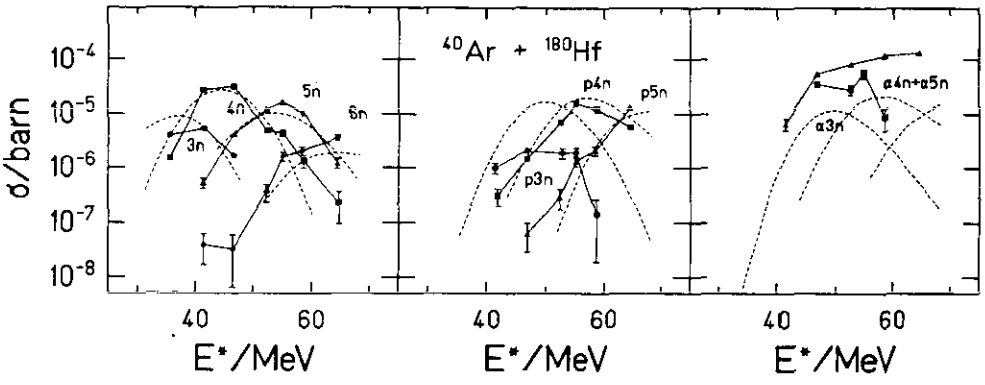

Figure 23. Evaporation-residue cross sections measured in the reaction ^{40}Ar + ^{180}Hf (Vermeulen *et al* 1984). The broken curves give the result of an evaporation calculation using standard parameters. However, a strong shell damping (E_d = 6 MeV) was used, and the liquid-drop fission barriers were slightly adjusted in order to better reproduce the cross sections of the xn channels. The full lines are drawn to guide the eye. From Vermeulen *et al* (1984).

The strongly varying shell effect in the ground state of these thorium nuclei is demonstrated in figure 24 by the differences of the experimental masses (Wapstra *et al* 1988) or the semi-empirical mass description of Liran and Zeldes (1976) and the liquid-drop masses (Möller and Nix 1981b). Although the masses of the neutron-deficient isotopes have not yet been measured, the semi-empirical description is probably rather exact, since the measured α-decay energies of the nuclei in this region are very well reproduced. As a consequence, the fission barriers which are indicated in figure 24 by the sum of the liquid-drop prediction (Dahlinger *et al* 1982) and the ground-state shell correction are expected to reflect the same structure. This simple estimate of the fission barrier is suggested by figure 17 and essentially corroborated

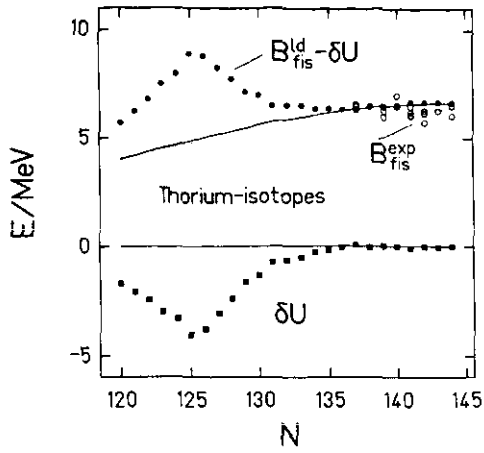

Figure 24. Lower part: ground-state shell effects δU of thorium isotopes, calculated as the difference of the experimental masses (Wapstra *et al* 1988) or the semi-empirical masses (Liran and Zeldes 1976) and the liquid-drop masses (Möller and Nix 1981*b*). Upper part: The open points correspond to the measured fission barriers B^{exp}_{fis} (taken from Dahlinger *et al* 1982). An estimate of the fission barriers (full points) is given by the difference of the liquid-drop fission barriers B^{ld}_{fis} (full curve, Dahlinger *et al* 1982) and the ground-state shell effects δU. The dotted curve shows the fission barriers predicted by the finite-range liquid-drop model of Sierk (1986) for comparison.

by Patyk *et al* (1988). Only for nuclei with almost vanishing liquid-drop fission barrier this estimate overpredicts the fission barrier substantially (Patyk and Sobiczewski 1990). The prediction of the finite-range liquid-drop model of Sierk (1986) is also shown for comparison.

In addition to the evaporation residues, fission products have been measured for the ^{40}Ar-induced reactions. The fission cross sections are included in figure 33. By assuming that all fission events are preceded by a fusion reaction, these data revealed that the maxima of the 4n channels occur somewhat above the respective fusion barriers for all systems. Therefore, these maximum values traced as a function of the neutron number of the compound nucleus (figure 25) can be taken as a probe of the influence of the shell stabilization on the fission competition in the de-excitation process.

Figure 25 reveals a general tendency of the evaporation-residue cross sections to increase with increasing neutron excess of the compound nucleus. The data do not reflect the structure in the fission barriers around $N = 126$ as shown in figure 24. For a quantitative analysis of these data, the result of an evaporation calculation is included in figure 25, at which the parameters were set to the standard values as defined in section 4.2. However, the collective contributions to the level density are not included. We refer to section 4.5.1 for a discussion on this subject.

Obviously, there is a huge discrepancy; the calculated cross sections are much too high, and near $N = 126$ they show a bump which is not observed. The calculated cross sections are particularly sensitive to the liquid-drop fission barriers which were taken from the empirical liquid-drop description of Dahlinger *et al* (1982) and to the shell effects in the level density which were washed out according to expectations from microscopic calculations with an exponential function by use of a damping constant of about 20 MeV as predicted by relation (4.8). The data are rather well

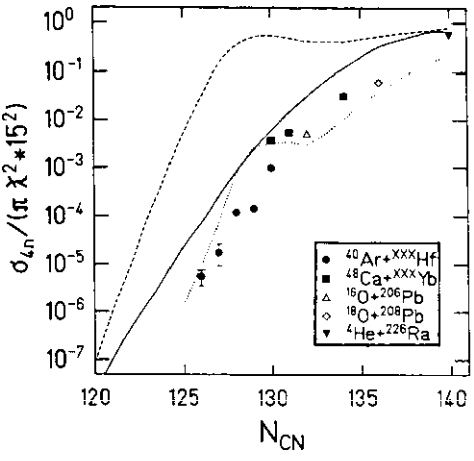

Figure 25. Maximum cross sections of the 4-neutron evaporation channel measured in different mass-asymmetric reactions (see inset) as a function of the neutron number of the compound nucleus. By dividing the cross sections by $15^2 \times \pi\,\lambda^2$, the ordinate corresponds approximately to the survival probability w for central collisions (Schmidt *et al* 1980). Broken curve: evaporation calculation using standard parameters. Full curve: evaporation calculation using nuclear liquid-drop properties only. Dotted curve: evaporation calculation with rotational levels included. For details see text. Data from Vandenbosch and Seaborg (1958), Häusser *et al* (1973), Bonin (1983), Vermeulen *et al* (1984) and Sahm *et al* (1985).

reproduced by a somewhat curious calculation which uses liquid-drop masses (Myers and Swiatecki 1967) and liquid-drop fission barriers (Dahlinger *et al* 1982) as well as level densities without microscopic corrections. Almost the same result is obtained from the first-mentioned calculation with experimental masses and realistic fission barriers (figure 24), however, by reducing the shell-damping constant E_d in the level-density description to 6 MeV. This value is in clear contradiction with theoretical expectations (see section 3.2).

The experimental findings in this unique test case, where highly fissile nuclei with a well-localized shell effect could be investigated, make it necessary to re-examine the theoretical ideas about the influence of shell effects on the fission competition in the de-excitation process which can be traced back to shell effects on the nuclear level density.

4.5. Mechanisms for a strong damping of shell effects in the nuclear level density

In order to explain the almost complete absence of a stabilizing influence of the 126-neutron shell on the cross sections of thorium residues, a careful study of nuclear properties which have some impact on the nuclear level densities was made. This study resulted in essentially two ideas which will be presented in the following subsections.

4.5.1. Temperature-induced deformation. The enhancement of the nuclear level density due to collective motion strongly depends on the nuclear structure; while in magic spherical nuclei essentially only vibrational motion is observed, the level density of deformed nuclei is much more enhanced due to the contribution of rotational bands. Transitional nuclei show an intermediate behaviour. Thus, the expected stabilizing

influence of the higher fission barriers of nuclei near $N = 126$ on the survival probability against fission is counteracted by the lower collective enhancement of the level density which reduces the statistical weight of the particle evaporation for these nuclei. Ignatyuk *et al* (1983) suggested that the influence of nuclear structure on the collective enhancement in the level density might be strong enough to counterbalance the expected structural effects in the intrinsic level density and to explain the observed lack of shell structure in the 4n cross sections of thorium isotopes as shown in figure 25.

It is obvious that the nucleus is not restricted to its ground-state shape. Due to phase-space arguments, the most probable shape of an excited nucleus is essentially determined by the highest level density and no longer by the lowest potential energy (Moretto and Stella 1970). Moretto (1972a, 1974) as well as Brack and Quentin (1974) studied the intrinsic level density as a function of deformation and found that nuclei which are deformed in their ground state tend to be spherical when they are excited because shell effects which determine the ground-state deformation are smeared out with increasing temperature. Vigdor and Karwowski (1982) as well as Schmidt *et al* (1984a) extended these considerations by the inclusion of the collective enhancement. Its energy dependence was introduced according to theoretical estimations. With increasing excitation energy, the collective motion is expected to be damped into the intrinsic background when the nuclear temperature approaches the single-particle Coriolis excitation (Bohr and Mottelson 1975), and the collective enhancement of the level density disappears. Bjørnholm *et al* (1974) deduce a limiting excitation energy

$$E^*_{\mathrm{lim}} = 200A^{1/3}\delta^2 \text{ MeV} \tag{4.14}$$

for the rotational enhancement which depends on the nuclear deformation δ. This means that the rotational enhancement persists up to about 100 MeV in a substantially deformed ($\delta \approx 0.3$) heavy nucleus.

Figure 26 shows the predicted level density as a function of excitation energy and quadrupole deformation for two nuclei, namely ^{216}Th which is spherical in its ground state and ^{252}Fm which is deformed. We conclude that the gain in level density due to rotational levels leads to a temperature-induced deformation which inevitably destroys the spherical $N = 126$ shell effect on the competition between fission and particle evaporation. The deformation of ^{252}Fm, however, is changed only little. In figure 25, the result of an evaporation calculation is included in which the level density in the statistically most favoured deformation is used for each evaporation step. The predicted influence of the $N = 126$ shell on the fission competition is very much reduced. In spite of this success, another problem emerges: while the calculation with the intrinsic level density using a strong shell damping ($E_d = 6$ MeV) reproduces the excitation functions of the neutron-evaporation channels in a satisfactory way, the calculated slope of the total neutron-evaporation cross section as a function of energy is too steep above the fusion barrier when the rotational levels are included. This can be understood by the different rotational enhancements due to the different moments of inertia at the fission saddle and in the ground state. A reduction of the ratio $a_{\mathrm{fis}}/a_{\mathrm{n}}$ with respect to the value deduced from relation (4.10) or a dissipative limitation of fission higher than expected would tend to reduce this discrepancy.

We come to the conclusion that it is essential to include the whole deformation space of the nucleus in order to evaluate the statistical weight of a specific de-excitation channel. The collective enhancement of the level density as described by

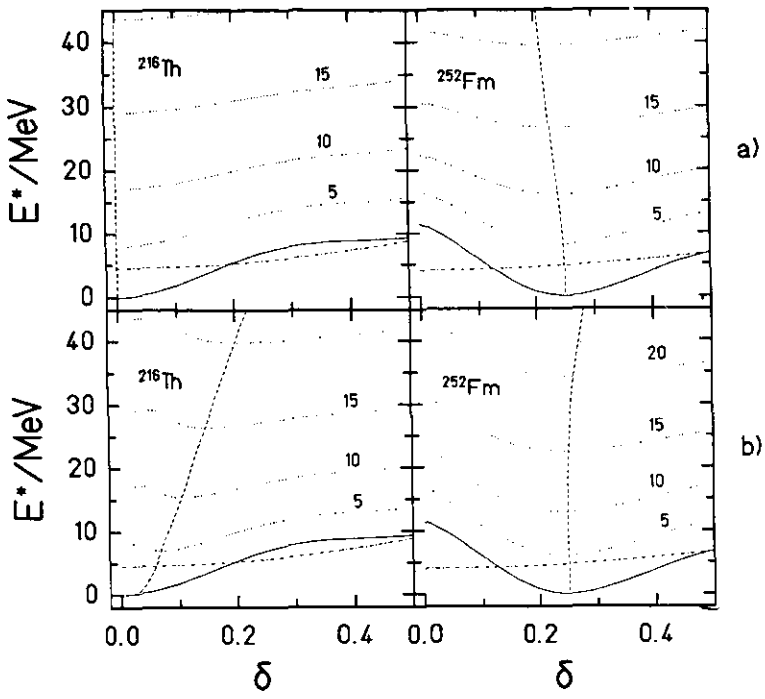

Figure 26. Calculated nuclear level density (a) without and (b) with the inclusion of rotational levels for a spherical (^{212}Th) and a deformed nucleus (^{252}Fm). The dotted contour lines are labelled with the nuclear level density ($\log_{10}(\rho/\mathrm{MeV}^{-1})$) for zero angular momentum. The broken curve connects the configurations with a maximum level density for a given excitation energy. The full curve is the deformation-dependent potential. The chain curve represents the liquid-drop potential. From Schmidt *et al* (1984a).

theoretical models (Bjørnholm *et al* 1974, Hansen and Jensen 1983, Maino *et al* 1990) leads to a temperature-induced deformation, while the intrinsic level density alone would favour the spherical shape. By this effect, spherical shell effects in the nuclear level density disappear at rather low excitation energies whereas deformed shells remain nearly unchanged. Unfortunately, besides the weak stabilizing influence of the 126 neutron shell on the cross sections of thorium residues, no direct experimental proof for this effect is available. In this context it is interesting to note that in measured γ spectra and angular distributions, indications for a substantial deformation of highly excited nuclei have been found (Snover 1986, 1988, Gaardhoje *et al* 1986, Gundlach *et al* 1990). However, up to now they have been interpreted in terms of angular-momentum-induced shape changes as predicted by the rotating-liquid-drop model (Cohen *et al* 1974) and in terms of shape fluctuations (Levit and Alhassid 1984, Gallardo *et al* 1985, 1987, Goodman 1988, Alhassid and Bush 1990).

4.5.2. Mutual support of magicities. As already mentioned in section 4.2.2, the microscopic calculation of the intrinsic level density relies on the single-particle level scheme. We therefore want to investigate the single-particle levels in some detail. There are two direct sources of information on the energies of the single-particle levels, namely the spectroscopy of excited levels and the binding energies of neutrons

and protons in the nucleus.

Systematic studies of spectroscopic information (see e.g. Hamilton *et al* 1985) reveal that the single-particle levels vary their position in energy as a function of the occupation considerably. In particular, the sequence of proton single-particle levels has been found to change when the neutron number in the nucleus is changed and vice versa. Some states even travel across a major closed shell and appear as intruder states at the 'wrong side' of the shell gap.

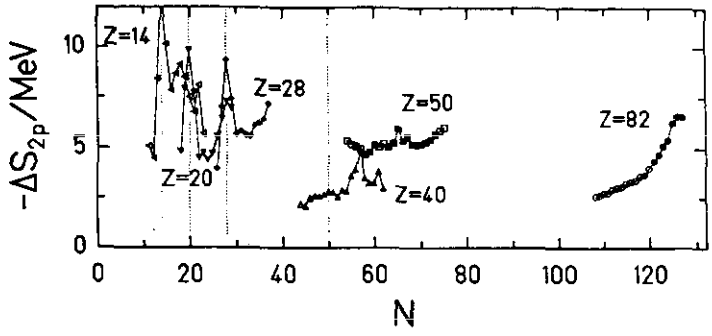

Figure 27. Two-proton separation energies $\Delta S_{2p} = S_{2p}(Z+2,N) - S_{2p}(Z,N)$ across proton shells as a measure of the proton shell gap drawn as a function of neutron number N. Full symbols: values deduced from measured masses, open symbols: values deduced from systematics, both taken from (Wapstra *et al* 1988). In most mass predictions, the shell gaps are assumed to be constant. Only by introducing a strong neutron–proton residual interaction (Zeldes *et al* 1983) can the observed drastic variations be reproduced. The values for $N = Z$ which are reached for light nuclei are increased by the Wigner term in the nuclear binding energy (see e.g. Myers 1977).

The shell gap in the single-particle level scheme can be deduced from separation-energy differences. In the independent-particle model where residual interactions are neglected, the energy gap of a neutron shell is given by

$$G_n(Z,N) = -\tfrac{1}{2}(S_{2n}(Z,N+2) - S_{2n}(Z,N)). \tag{4.15}$$

$S_{2n}(Z,N)$ is the two-neutron separation energy of the nucleus with Z protons and N neutrons. This quantity avoids the even–odd structure in the masses. In an analogous way, the energy gap of a proton shell can be deduced from the two-proton separation energies $S_{2p}(Z+2,N)$ and $S_{2p}(Z,N)$. A systematic study of α-decay energies (Schmidt *et al* 1979) and two-particle separation energies (Schmidt and Vermeulen 1980) revealed that the nuclei show a general tendency for a mutual support of magicities. That means that a specific proton shell gap is maximum in nuclei which have a magic neutron number and vice versa. Figures 27 and 28 show an updated version of this study. The clear signature of the mutual support of magicities is striking. All shell gaps are very much influenced by the occupation of the other kind of nucleons. This variation of the single-particle energies with occupation number may be caused by configuration mixing in nuclei (De Shalit and Goldhaber 1953). The observed effect around ^{208}Pb has quantitatively been interpreted by Zeldes *et al* (1983) in terms of a residual interaction between neutrons and protons in specific orbits. Thus, the modification of the single-particle energies is caused by the variation of the occupation of specific orbits and not by a global variation of the size or the shape of the nuclear potential.

In this context, it is important to keep in mind that the level density as calculated by microscopic models is based on a single-particle level scheme which is assumed to be independent of excitation energy. In this way, the shell-damping energy of about 20 MeV was estimated for heavy nuclei by relation (4.9). In contrast to this assumption, we noticed that any shell gap is drastically reduced with increasing number of particles or holes outside a doubly-magic configuration. These seem to destroy the 'symmetry' realized in doubly-magic nuclei more than expected in the independent-particle model. This leads to the expectation that the smearing of the occupation function around the Fermi surface due to increasing temperature has a similar influence. Thus, the estimated shell-damping energy can only be considered as an upper limit. However, this additional reduction of shell effects in the level density cannot quantitatively be estimated before the observed effects of the residual interactions like the energy position of intruder states or the mutual support of magicities are better understood. There is hope for considerable progress in the understanding of these residual interactions due to the efforts currently made (Hamilton *et al* 1985). The mutual support of magicities was already included in the semi-empirical mass prediction of Liran and Zeldes (1976) and was explicitly considered in a recent mass formula (Tachibana *et al* 1988).

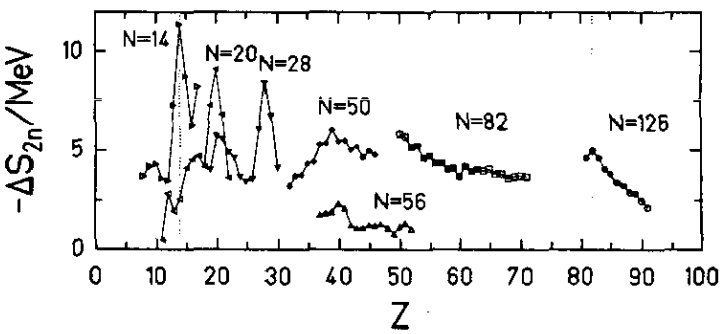

Figure 28. Two-neutron separation energies $\Delta S_{2n} = S_{2n}(Z, N+2) - S_{2n}(Z, N)$ across neutron shells as a measure of the neutron shell gap drawn as a function of proton number Z. See figure 26 for details.

We conclude that the observed weak enhancement of the survival probability in the de-excitation process of shell-stabilized spherical nuclei can qualitatively be understood by the influence of the temperature-induced deformation and the mutual support of magicities. The thorium isotopes across the $N = 126$ neutron shell have the advantage of showing a strongly-varying shell effect in a short isotopic sequence. These nuclei are expected to be all spherical or only slightly deformed just like those around $N = 184$, whereas the nuclei well above the $N = 126$ shell up to the heaviest known nucleus $^{266}109$ are all deformed. The study of shell effects in heavy deformed nuclei and their influence on the fission competition would be much more difficult, because there the shell effects vary more gradually as a function of the nucleon number so that their influence on evaporation-residue cross sections could not be disentangled easily from the macroscopic trends.

5. Indications for a direct coupling between entrance channel and de-excitation phase

In the preceding sections, the clear division of the fusion process and the de-excitation phase by assuming the formation of a compound nucleus allowed us to extract separate information on the fusion and on the de-excitation. In this section, we will give a survey on those theoretical ideas and experimental information which call this assumption into question.

There are essentially two processes known in the literature which could lead to deviations from the statistical model. The first one is the emission of particles before the energy of the composite system is equilibrated. These particles have higher kinetic energies than expected in the statistical model. Precompound emission of highly energetic particles is only expected for considerable relative velocities of the reaction partners at the barrier (Blann 1985, Iwamoto 1987, Fabrici *et al* 1989). It should not play any role in the synthesis of heavy nuclei at energies near the potential barrier. The second one is the dissipation during the strong shape variation from the ground state to the fission-barrier configuration. This dissipative process tends to reduce the fission width with respect to the statistical value. As already mentioned, the dissipative limitation of fission was found to manifest itself in the observation of high rates of prescission particles (Hinde *et al* 1989) only at excitation energies in excess of about 50 MeV. From these arguments one does not expect any deviation from the statistical model at energies around the fusion barrier for the most massive systems. However, we would prefer a direct experimental indication. Therefore, we will check the available experimental information in some detail.

The energy spectra of evaporated charged particles and γ rays were extensively measured for systems around $^{90}Zr + {}^{90}Zr$ and were found to be in accordance with the predictions of the statistical model (see section 4.3). Such detailed experimental information could not be obtained for more massive systems because the onset of the extra-push phenomenon goes in line with an increasing fission competition in the de-excitation process, resulting in considerably lower evaporation-residue cross sections. For these systems, however, the validity of the statistical model may still be tested by comparing the cross sections of evaporation residues formed in different projectile–target combinations which lead to the same composite system. If all reactions pass by the formation of a compound nucleus, the competition between different evaporation channels will not depend on the entrance channel. Such a test was made e.g. by comparing the two projectile–target combinations, $^{40}Ar + {}^{180}Hf$ and $^{124}Sn + {}^{96}Zr$, which both lead to the composite system ^{220}Th. The fission competition in the de-excitation process, which increases with increasing angular momentum, is expected to limit the angular-momentum range which leads to evaporation-residue formation, and thus it is expected to eliminate any influence of the different spin distributions populated in the different fusion reactions. Figure 29 shows that the relative intensities of the neutron- and proton-evaporation channels give no indication for reactions which do not pass by a compound nucleus, within the experimental uncertainly. The evaporation of α particles seems to be enhanced in the more asymmetric systems. However, this difference is hardly significant due to the uncertainty of the transmission of SHIP. Therefore, we will look for a more stringent test.

In a series of experiments, a complete survey was performed on the evaporation residues formed in three different systems, $^{110}Pd + {}^{100}Mo$, $^{110}Pd + {}^{104}Ru$, and $^{110}Pd + {}^{110}Pd \rightarrow {}^{220}U$ (Morawek 1991). In figure 30, the measured cross sections are compared with the expected values as calculated with the statistical model on a

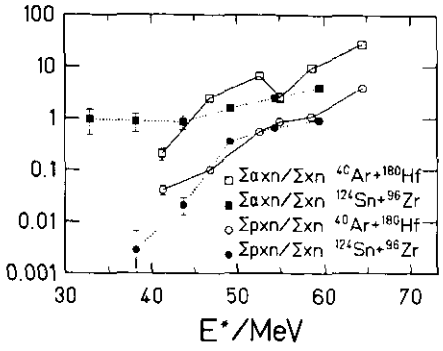

Figure 29. Ratios between different classes of evaporation residues as indicated, measured in a mass-asymmetric (^{40}Ar+^{180}Hf) and an almost mass-symmetric (^{124}Sn+^{96}Zr) system, are shown as a function of the excitation energy of the compound nucleus ^{220}Th. In addition to the statistical errors presented by the error bars, the not exactly known transmission of SHIP causes an uncertainty of a factor of two on the ratio $\sum \alpha xn / \sum xn$ and of about 30% on the ratio $\sum pxn / \sum xn$.

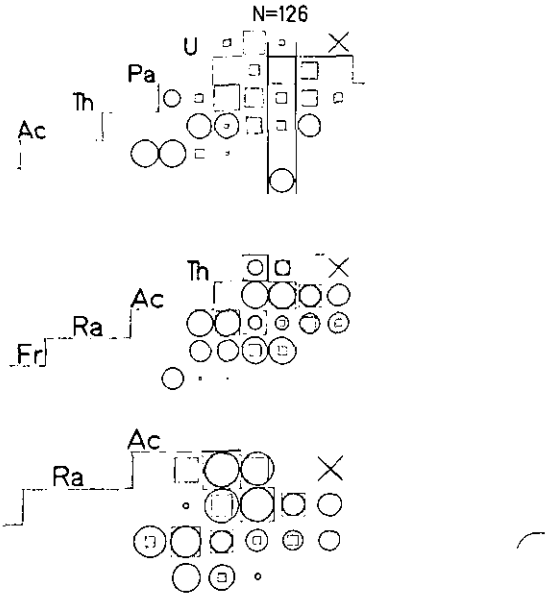

Figure 30. Measured (circles) and calculated (squares) cross sections of evaporation residues in the reactions ^{110}Pd + ^{100}Mo (E^* = 43 MeV), ^{110}Pd + ^{104}Ru (E^* = 40 MeV), and ^{110}Pd + ^{110}Pd (E^* = 39 MeV) (Morawek 1991). The diameters of the symbols are proportional to the logarithm of the cross sections. The compound nucleus is indicated by a cross. The parameters of the evaporation calculation were fixed to the standard values as defined in section 4.2, except that the shell-damping energy E_d was reduced to 6 MeV.

chart of nuclides. Due to the limitation to almost central collisions by the angular-momentum-dependent fission competition, the fusion cross section is expected to act as a common scaling factor, whereas the relative magnitudes of the different evaporation channels are determined by the evaporation stage. While the experimental and

the calculated distributions agree well for the lightest system, there is a drastically increasing discrepancy for the heavier systems. The evaporation of charged particles is much stronger than expected. This finding is confirmed by figure 31, where the measured and the calculated values for the formation of different elements are compared. The parameters of the statistical-model calculation are fixed to the values which are able to reproduce the detailed experimental information on cross sections, charged-particle spectra, and γ spectra for the systems $^{90}Zr + {}^{90}Zr$, ^{89}Y (Keller *et al* 1986, Schmidt *et al* 1986, Gollerthan *et al* 1991). The fission barriers were taken from the empirical description of Dahlinger *et al* (1982), and the shell-damping constant $E_d = 6$ MeV was applied in the level-density formula (4.7) in order to effectively account for the observed fragility of the $N = 126$ shell effect.

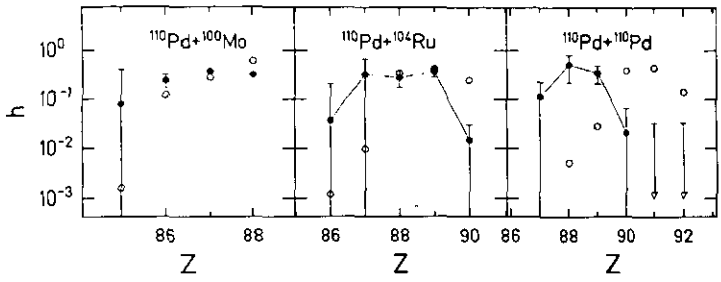

Figure 31. Measured (full points and arrows) and calculated (open points) normalized element distributions from the data shown in figure 29.

By extending the model of Grangé and Weidenmüller (1980) and Grangé *et al* (1983) to the first reaction phase, Morawek (1991) introduced the idea that light particles may already be emitted during the dynamic evolution from contact towards amalgamation. The change in the nuclear composition would have an impact on the subsequent dynamic evolution. In particular, the repulsive electrostatic force would be reduced by the emission of charged particles. As a consequence, the extra-push would also be reduced, and those reactions would lead to fusion with a higher probability.

Morawek considered the evaporation of particles from the strongly deformed system before it is captured inside the fission barrier by assuming that the energy on the dynamic path above the potential (figure 11) is immediately thermalized. The reaction time was deduced from dynamical calculations (Błocki *et al* 1986). In the reaction $^{110}Pd + {}^{110}Pd$ at $E = 284$ MeV, Morawek estimated the probability of the system evaporating an α particle before it reaches a configuration near the fission barrier to be of the order of 10^{-4}. This value, multiplied with the survival probability of the daughter nucleus ^{216}Th which can be deduced from the measured cross sections of the system $^{40}Ar + {}^{176}Hf$ is able to reproduce the total amount of evaporation residues observed in the reaction $^{110}Pd + {}^{110}Pd$. This picture corresponds to the extreme assumption that the system $^{110}Pd + {}^{110}Pd$ does not fuse at all, while the loss of an α particle on the early reaction stage leads to fusion with high probability. This model explains that *no xn* and *pxn* channels were observed for the most massive system. Although this model is certainly too schematic, it stresses the importance of the interplay between dynamical evolution and particle evaporation in the fusion of very massive systems.

Motivated by the measured element distributions for the most massive systems,

the relevance of well-established theoretical models to the entire reaction was re-examined. This study revealed that the assumed division of the synthesis process in a first stage which describes the dynamical evolution leading to the formation of a compound nucleus and a second subsequent statistical de-excitation stage is severely called in question. As a consequence, the synthesis process of a very massive system can be considered only as a whole. This complicates very much the quantitative theoretical understanding of evaporation-residue cross sections for very massive systems.

6. Conclusions with respect to the synthesis of the heaviest nuclei

The heaviest nuclei can be synthesized only with extremely low cross sections. Therefore, direct studies on the characteristics of these reactions are more difficult than those presented in the preceding sections, which led to composite systems between mercury and uranium. Nevertheless, by use of nearly symmetric systems, similar values for the Coulomb repulsion in the entrance channel could be reached to those encountered in the synthesis of heavy elements, while the fission competition in the de-excitation process was less severe. In this last section, we will show that many of the characteristics found in the studies which were presented above help to understand the characteristics and to determine the optimum conditions for the synthesis of the heaviest nuclei.

6.1. The projectile–target combination

Our first consideration concerns the impact of the projectile–target combination on the conditions for the production of heavy elements. The synthesis of the heaviest nuclei by fusion reactions has first been performed with rather asymmetric projectile–target combinations by using the heaviest targets available (e.g. Flerov *et al* 1964, Ghiorso *et al* 1969, 1970b, 1974). Compound nuclei with lower excitation energies were produced in more symmetric systems by use of targets in the vicinity of the doubly-magic ^{208}Pb (Oganessian 1974). The combination of ^{208}Pb with the doubly-magic ^{48}Ca resulted in exceptionally high evaporation-residue cross sections (Orlova *et al* 1978, Nitschke *et al* 1979). Figure 32 summarizes the empirical information on the maximum element production cross sections accumulated in Berkeley, Dubna and Darmstadt for rather mass-asymmetric actinide-based reactions and those using targets near ^{208}Pb. Although the more symmetric systems aim at more neutron-deficient and thus more fissile compound nuclei, they give the highest production cross sections for the heaviest elements. We are now able to attribute these findings to the Q value of the reaction (Oganessian 1974) and to nuclear-structure effects on the hindrance to fusion (Sahm *et al* 1985, Armbruster 1987, Quint *et al* 1991). Both the high negative reaction Q value and the reduced barrier shift expected for magic reaction partners tend to increase the evaporation-residue cross sections. While Flerov and Ter-Akopian (1987) report on possible evidence for the formation of element 110 in ^{40}Ar and ^{44}Ca-induced reactions, all attempts to synthesize superheavy nuclei with $Z > 110$ have failed up to now (see Flerov and Ter-Akopian 1983, Kratz 1985). Two constraints make these attempts very difficult: in rather mass-symmetric systems one expects a drastic hindrance to fusion (section 3.5), whereas in more mass-asymmetric systems the chances for fission are increased due to the higher excitation energies at the potential barrier (section 3.2).

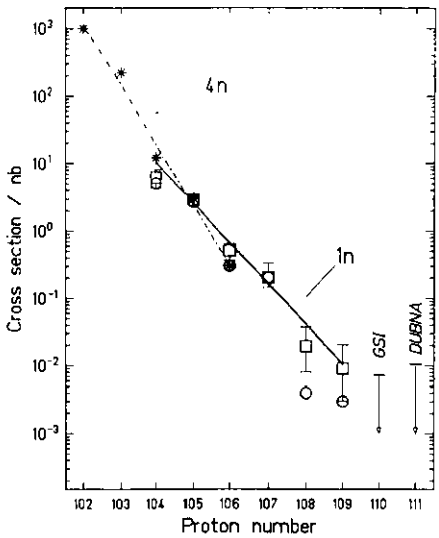

Figure 32. Cross sections for the production of the heaviest elements. Asterisks: actinide-based reactions (4n channels); circles: cold fusion (1n channel) measured in Dubna; squares: cold fusion (1n channel) measured in Darmstadt. The data originate from Oganessian *et al* (1984), Hessberger *et al* (1985a, b), Münzenberg *et al* (1981, 1984a, 1985) and Ghiorso *et al* (1969, 1970a, 1974). The figure is taken from Münzenberg (1988).

The use of radioactive projectiles which are becoming available as secondary beams could help to produce more neutron-rich composite systems with larger values for the difference of fission barrier and neutron binding energy $B_{fis} - B_n$. For these systems a higher survival probability in the de-excitation process is expected. A severe limitation, however, is the intensity of secondary beams which is considerably reduced compared with stable beams.

6.2. The bombarding energy

Another important parameter for the synthesis process is the bombarding energy. If the fusion is hindered, the mean effective fusion barrier is increased with respect to the one-dimensional potential barrier. One could therefore suspect that this energy shift has to be considered when optimum conditions for the synthesis of heavy elements are to be attained.

However, the below-mentioned observations are in contradiction to this expectation. A systematic study (Clerc *et al* 1984) of measured cross sections for evaporation residues and fission-like products in a series of reactions from $^{40}Ar + ^{165}Ho \rightarrow ^{205}At$ to $^{50}Ti + ^{209}Bi \rightarrow ^{259}105$ revealed that the energy where a maximum in the evaporation-residue cross section is observed nearly coincides for all systems with the calculated one-dimensional potential barrier B_{Bass} using the empirical nuclear potential of Bass (1980). Figure 33 shows an updated extension of this study which proves that this statement even holds for the reactions $^{45}Cr + ^{208}Pb$, $^{54}Cr + ^{209}Bi$ and $^{58}Fe + ^{208}Pb$, aiming at the elements 106, 107 and 108. This finding is even more surprising as for one of the reactions ($^{50}Ti + ^{208}Pb$), Hessberger *et al* (1985b) deduced a considerable shift of the mean fusion barrier of (21 ± 3) MeV with respect to the expected one-dimensional potential barrier by comparing the evaporation-residue cross section with that measured in the asymmetric system $^{12}C + ^{249}Cf$ (Ghiorso *et al* 1969, Bemis *et al*

1973, Eskola *et al* 1970). Only the synthesis of the heaviest nucleus observed until now in the reaction ^{209}Bi(^{58}Fe, n)^{266}109 (Münzenberg *et al* 1984b, 1988) was achieved at an energy 5 MeV above the expected potential barrier B_{Bass}.

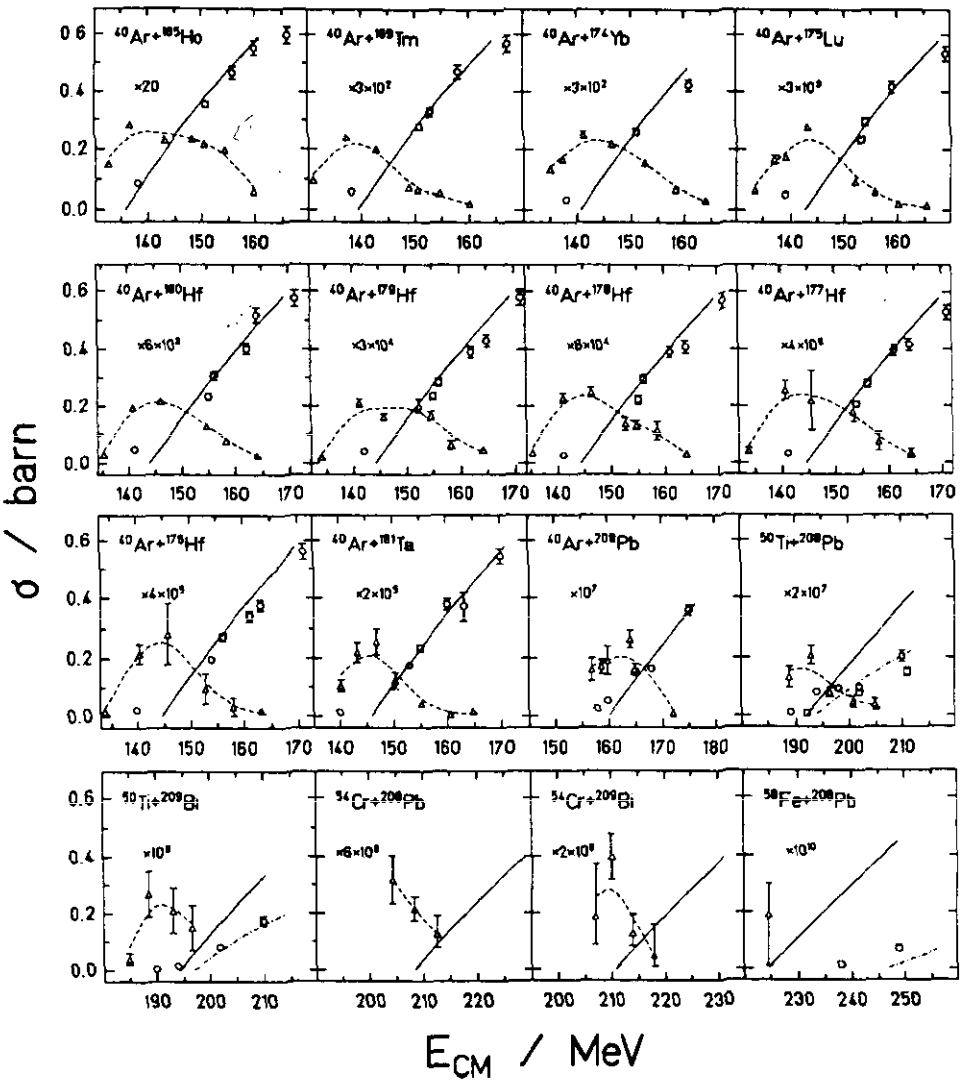

Figure 33. Cross sections for fission and neutron-evaporation residues for compound systems between ^{205}At and ^{266}108. The open triangles denote the evaporation-residue data. The broken curves are drawn to guide the eye. The open circles and squares represent the measured cross sections for fission-like events. The thick full curves are standard predictions for the fusion cross section with the Bass potential (Bass 1980) without tunnelling. The chain curves correspond to fusion cross sections as calculated from the extra-push model (Swiatecki 1981). The data are taken from Clerc *et al* (1984) and Münzenberg (1988).

For a closer view on this subject we remind the reader that the fusion probability generally increases with energy until it saturates slightly above the mean effective

barrier (see figures 7 and 8) while the survival probability decreases nearly exponentially with energy (see section 4.1). The maximum of the evaporation-residue cross section occurs at that energy at which the logarithmic slope of the increasing fusion probability is equal to the absolute value of the logarithmic slope of the decreasing survival probability.

In the one-dimensional fusion model, the fusion probability as given by the transmission coefficient of a single potential barrier changes its slope from an almost exponential behaviour below the barrier to saturation above the barrier in a narrow energy range. In this case, the energy position of the maximum of the evaporation-residue cross section is reached close to the potential barrier. For the heavy systems, however, the fusion probability is expected to vary more gradually with energy, in particular when the fusion is hindered (see figure 10). Only below the adiabatic barrier, the steep slope of the tunnelling regime is reached. As the slope of the survival probability for very fissile nuclei is very steep, the maximum evaporation-residue cross section is shifted to energies below the mean effective fusion barrier, in the extreme it may coincide with the adiabatic barrier. This adiabatic barrier was found to be near the calculated one-dimensional potential barrier for the most massive symmetric systems which showed an appreciable hindrance to fusion (section 3.5). Thus, the fact that the heaviest nuclei were also synthesized at incident energies near the calculated one-dimensional potential barrier is by no means an indication for an unhindered fusion process.

Figure 33 shows that the measured cross sections of fission-like events are well described by considering the passage over the one-dimensional potential barrier B_{Bass} with the exception of the heaviest systems which show a reduced slope of the fission excitation function. It is puzzling that even for the heaviest systems shown in figure 33 the passage over the one-dimensional potential barrier is sufficient for fission-like events to be produced in central collisions while the formation of evaporation residues was found to be strongly hindered at near-barrier energies (Hessberger *et al* 1985b). This finding could be an indication that the heaviest nuclear systems most probably develop towards immediate reseparation in the later dynamic evolution while the neck is formed (see figure 11). Due to the fluctuation on the dynamic path, a small part of the reactions is captured inside the fission barrier and may lead to evaporation-residue formation whereas the bulk part ends up in fast-fission events.

6.3. The limits for the synthesis of heavy nuclei

Even if the most favourable conditions are chosen, the synthesis of heavy nuclei seems to be finally limited by several effects. Most of them can be traced back to the electrostatic repulsion in the dynamic evolution of the system. In the following we will give a survey of the present understanding of these effects.

In more and more massive systems a larger overlap of the density distributions of the reaction partners is needed to reach the potential barrier because the larger Coulomb repulsion can only be balanced by a stronger nuclear force. This tends to increase the energy transfered to friction and to diabatic excitations until the potential barrier is reached. The fluctuation phenomena in these processes still allow a compact configuration inside the potential barrier to be reached with a bombarding energy close to the calculated one-dimensional potential barrier, however, with a small probability. In the following reaction stage, the dynamic evolution and the de-excitation process might overlap in time and influence each other as suggested by the observations in the system ^{110}Pd + ^{110}Pd. The evaporation of charged particles

during the amalgamation may increase the fusion probability, however, it also tends to limit the nuclear charge of the evaporation residues to be reached.

The heaviest nuclei synthesized up to now are stabilized against spontaneous fission by shell effects only (Patyk *et al* 1988). The same is expected for even heavier nuclei. The synthesis process profits only little from this stabilization, because the nuclear system is heated up. Both the dynamic evolution and the de-excitation are dominated by the liquid-drop trend which drives the system towards reseparation and fission, respectively. Therefore we expect that the synthesis of elements beyond element 109 becomes increasingly more difficult; at some point it will be impossible within reasonable time with the present experimental technique. The formation cross sections will probably decrease further with increasing fissility of the composite system. Due to the extraordinary fragility of spherical shell effects in the nuclear level density (section 4.5) we expect an even steeper descent of the formation cross sections when the composite system approaches the $N = 184$ shell, although the shell effects are predicted to increase (e.g. Patyk and Sobiczewsky 1990).

The systematic studies on the conditions for the synthesis of heavy nuclei presented in this review have increased the knowledge of the reaction aspects considerably. One result of these studies is an ever-increasing complexity for more and more massive systems. The available theoretical models explain several aspects of the observed characteristics, but they each treat only a different part of the reaction. We hope that the accumulated experimental information will stimulate the development of still more elaborate theoretical models.

Acknowledgments

Helpful comments from P Armbruster, H-G Clerc, E Hanelt and G Münzenberg are gratefully acknowledged. We would also like to thank M Steiner for reading the manuscript.

References

Aguiar C E, Aleixo A N, Barbosa V C, Canto L F and Donangelo R 1989a *Nucl. Phys.* A **500** 195–211
Aguiar C E, Barbosa V C, Canto L F and Donangelo R 1987 *Nucl. Phys.* A **472** 571
—— 1988 *Phys. Lett.* **201B** 22–4
Aguiar C E, Barbosa V C, Donangelo R 1990 *Nucl. Phys.* A **517** 205–20
Aguiar C E, Barbosa V C, Donangelo R and Souza S R 1989b *Nucl. Phys.* A **491** 301–13
Alexander J M, Magda M T and Landowne S 1990 *Phys. Rev.* C **42** 1092–8
Aljuwair H, Ledoux R J, Beckerman M, Gazes S B, Wiggins J, Cosman E R, Betts R R, Saini S and Hansen O 1984 *Phys. Rev.* C **30** 1223–7
Alhassid Y and Bush B 1990 *Phys. Rev. Lett.* **65** 2527–30
Almqvist E, Bromley D A and Kuehner J A 1960 *Phys. Rev. Lett.* **4** 515–7
Almqvist E, Kuehner J A, McPherson D and Vogt E W 1964 *Phys. Rev.* **136** B84–98
Armbruster P 1985 *Ann. Rev. Nucl. Part. Sci.* **35** 135–94
—— 1987 *Scuola Int. di Fisica 'Enrico Fermi', Varenna, Italy* Lecture
Back B B 1985 *Phys. Rev.* C **31** 2104–12
Back B B, Betts R R, Gindler J E, Wilkins B D, Saini S, Tsang M B, Gelbke C K, Lynch W G, McMahan M A and Baisden P A 1985 *Phys. Rev.* C **32** 195–213
Balantekin A B, Koonin S E and Negele J W 1983 *Phys. Rev.* C **28** 1565–9
Bass R 1974 *Nucl. Phys.* A **231** 45–63
—— 1980 *Proc. Conf. on Deep Inelastic and Fusion Reactions with Heavy Ions, Berlin 1979* (Berlin: Springer) pp 281–93

Beckerman M 1985 *Phys. Rep.* **129** 145–223
—— *1988 Rep. Prog. Phys.* **51** 1047–103
Beckerman M, Ball J, Enge H A, Salomaa, M, Sperduto A, Gazes S, DiRienzo A and Molitoris J D 1981 *Phys. Rev.* C **23** 1581–9
Beckerman M, Salomaa M, Sperduto A, Enge H, Ball J, DiRienzo A, Gazes S, Yan Chen, Molitoris J D, Mao Nai-feng 1980 *Phys. Rev. Lett.* **45** 1472–5
Beckerman M, Salomaa M, Sperduto A, Molitoris J D and DiRienzo A 1982 *Phys. Rev.* C **25** 837–49
Beckerman M, Salomaa M, Wiggins J and Rohe R 1983 *Phys. Rev.* C **28** 1963–9
Beckerman M, Wiggins J, Aljuwair H and Salomaa M K 1984 *Phys. Rev.* C **29** 1938–41
Beghini S, Signorini C, Lundardi S, Morando M, Fortuna G, Stefanini A M, Meczynshi W and Pengo P 1985 *Nucl. Instrum. Methods* A **239** 585–91
Bellwied R, Kratz J V, Reisdorf W, Schüll D, Kohlmeyer P and Künkel R 1988 *Lecture Notes in Physics* **317** (Berlin: Springer) pp 125–30
Bemis C E 1974 *Proc. Int. Conf. on Reactions Between Complex Nuclei* vol 2, pp 529–44
Bemis C E Jr, Silva R J, Hensley D C, Keller O L Jr, Tarrant J R, Hunt L D, Dittner P F and Hahn R L 1973 *Phys. Rev. Lett.* **31** 647–50
Berdichevsky D, Lukasiak A, Nörenberg W and Rozmej P 1989 *Nucl. Phys.* A **499** 609–36
Berdichevsky D and Reisdorf W 1987 *Z. Phys.* A **327** 217–24
Berkowitz G M, Braun-Munzinger P, Korp J S, Freifelder R H, Renner T R and Wilschut H W 1983 *Phys. Rev.* C **28** 667–78
Bertsch G 1978 *Z. Phys.* A **289** 103–5
Bethe H A 1937 *Rev. Mod. Phys.* 9 67–244
Bhaduri R K and Das Gupta S 1973 *Phys. Lett.* **47B** 129–32
Bjørnholm S, Bohr A and Mottelson B R 1974 *Proc. Int. Conf. on the Physics and Chemistry of Fission, Rochester 1973* vol 1 (Vienna: IAEA) pp 367–74
Bjørnholm S and Swiatecki W J 1982 *Nucl. Phys.* A **391** 471–504
Blann M 1985 *Phys. Rev.* C **31** 1245–54
Blatt J and Weißkopf V F 1952 *Theoretical Nuclear Physics* (New York: Wiley)
Błocki J P, Feldmeier H and Swiatecki W 1986 *Nucl. Phys.* A **459** 145–72
Błocki J, Randrup J, Swiatecki W J and Tsang C F 1977 *Ann. Phys., NY* **105** 427–62
Bock R, Chu T, Dakowski M, Gobbi A, Grosse E, Olmi A, Sann H, Schwalm D, Lynen Y, Müller W, Bjørnholm S, Esbensen H, Wölfli W and Morenzoni E 1982 *Nucl. Phys.* A **388** 334–80
Bohr A 1936 *Nature* **137** 344–8
Bohr A and Mottelson B R 1975 *Nuclear Structure* vol 2 (New York: Benjamin)
Bohr N and Wheeler J A 1939 *Phys. Rev.* **56** 426–50
Bonin W 1983 private communication
Brack M and Quentin P 1974 *Phys. Lett.* **52B** 159–62
Brink D D 1955 *DPhil Thesis* Oxford University
Britt H C 1980 *Symp on Physics and Chemistry of Fission, Jülich, 1979* vol 1 (Vienna: IAEA) pp 3–27
Broglia R A, Dasso C H, Landowne S and Pollarolo G 1983a *Phys. Lett.* **133B** 34–8
Broglia R A, Dasso C H, Landowne S and Winther A 1983b *Phys. Rev. C27 2433–5*
Businaro U L and Gallone S 1957 *Nuovo Cimento* **5** 315–7
Canto L F 1989 *Nucl. Phys.* A **491** 337–48
Clerc H G, Keller H G, Sahm C C, Schmidt K H, Schulte H and Vermeulen D 1984 *Nucl. Phys.* A **419** 571–88
Cohen S, Plasil F and Swiatecki W J 1974 *Ann. Phys., NY* **82** 557–96
Cujec B and Barnes C A 1976 *Nucl. Phys.* A **266** 461–93
Dahlinger M, Vermeulen D and Schmidt K H 1982 *Nucl. Phys.* A **376** 94–130
Dayras R A, Stokstad R G, Switkowski Z E and Wieland R M 1976 *Nucl. Phys.* A **261** 478–90
Dasso C H, Landowne S and Winther A 1983 *Nucl. Phys.* A **405** 381–96
Dasso C H, Landowne S and Pollarolo G 1989 *Phys. Lett.* **217B** 25–7
Davies K T R and Sierk A J 1985 *Phys. Rev.* C **31** 915–22
Delagrange H, Grégoire C, Scheiter F and Abe Y 1986 *Z. Phys.* A **323** 437–49
De Shalit A and Goldhaber M 1953 *Phys. Rev.* **92** 1211–8
El Masri Y, Hanappe F, Steckmeyer J C, Martin V, Bizard G, Borderie B, Brou R, Bruandet J F, Duhamel P, Fuchs H, Laville J L, Péter J, Régimbart R, Rivet M, Tamain B and Tsang Ung Chan 1990 *Nucl. Phys.* A **517** 340–64
Ernst H, Henning W, Davids C N, Freeman W S, Humanic T J, Paul M, Sanders S J, Prosser F W Jr

and Racca R A 1982 *Phys. Lett.* **119B** 307–10
Esbensen H 1981 *Nucl. Phys.* A **352** 147–56
Eskola P, Eskola K, Nurmia M and Ghiorso A 1970 *Phys. Rev.* C **2** 1058–62
Fabrici E, Gadioli E, Gadioli Erba E, Galmarini M, Fabbri F and Reffo G 1989 *Phys. Rev.* C **40** 2548–57
Feldman W and Heikkinen D W 1969 *Nucl. Phys.* A **133** 177–212
Feldmeier H 1982 *Proc. Int. Workshop on Gross Properties of Nuclei and Nuclear Excitations, Hirschegg, Austria* pp 26–36
Fischer R D, Ruckelshausen A, Koch G, Kühn W, Metag V, Mühlhans R, Novotny R, Ströher H, Gröger H, Habs D, Heyng H W, Repnow R, Schwalm D, Reisdorf W and Simon R S 1986 *Phys. Lett.* **171B** 33–6
Fiset E O and Nix J R 1972 *Nucl. Phys.* A **193** 647–71
Flerov G N, Oganessian Yu Ts, Lobanow Yu V, Kusnetsov V I, Druin V A, Perelygin V P, Gavrilov K A, Tretiakova S P and Plotko V M 1964 *Phys. Lett.* **13** 73–5
Flerov G N and Ter-Akopian G M 1983 *Rep. Prog. Phys.* 46 817–75
—— 1987 *Prog. Part. Nucl. Phys.* **19** 197–239
Freeman W S, Ernst H, Geesaman D F, Henning W, Humanic T J, Kühn W, Rosner G, Schiffer J P, Zeidman B and Posser F W 1983 *Phys. Rev. Lett.* **50** 1563–6
Fröbrich P 1984 *Phys. Rep.* **116** 337–400
Fröbrich P and Richert J 1990 *Phys. Lett.* **237B** 328–33
Frömann N and Frömann P O 1965 *JWKB Approximation: Contributions to the Theory* (Amsterdam: North-Holland) chap 9
Gaardhoje J J, Ellegaard C, Herskind B, Diamond R M, Dekplanque M A, Dines G, Macchiavelli A O and Stephens F S 1986 *Phys. Rev. Lett.* **56** 1783–6
Gäggeler H, Sikkeland T, Wirth G, Brüchle W, Bögl W, Franz G, Herrmann G, Kratz J V, Schädel M, Sümmerer K and Weber W 1984 *Z. Phys.* A **316** 291–307
Gaimard J J and Schmidt K H 1991 *Nucl. Phys.* A submitted
Gallardo M, Diebel M, Døssing T and Broglia R A 1985 *Nucl. Phys.* A **443** 415–34
Gallardo M, Luis F J and Broglia R A 1987 *Phys. Lett.* **191B** 222–6
Ghiorso A, Nitschke J M, Alonso I R, Alonso C T, Nurmia M, Seaborg G T, Hulet E K and Lougheed R W 1974 *Phys. Rev. Lett.* **33** 1490–3
Ghiorso A, Nurmia M, Eskola K and Eskola P 1970a *Phys. Lett.* **32B** 95–8
Ghiorso A, Nurmia M, Eskola K, Harris J and Eskola P 1970b *Phys. Rev. Lett.* **24** 1498–503
Ghiorso A, Nurmia M, Harris K, Eskola K and Eskola P 1969 *Phys. Rev. Lett.* **22** 1317–20
Ghiorso A, Yashita S, Leino M, Frank L, Kalnins J, Armbruster P, Dufour J P and Lemmertz P K 1988 *Nucl. Instrum. Methods* A **269** 192–201
Gil S, Abriola D, DiGregorio D E, di Tada M, Elgue M, Etchegoyen A, Etchegoyen M C, Fernandez Niello J, Ferrero A M J, Macchiavelli A O, Pacheco A J, Testoni J E, Silveira Gomes P, Vanin V R, Charlop A, García A, Kailas S, Luke S J, Renshaw E and Vandenbosch R 1990a *Phys. Rev. Lett.* **65** 3100–3
Gil S, Vandenbosch R, Charlop A, García A, Leach D D, Luke S J and Kailas S 1990b preprint
Gil S, Vandenbosch R, Lazzarini A J, Lock D K and Ray A 1985 *Phys. Rev.* C **31** 1752–62
Gollerthan U 1988 *PhD Thesis* Inst. Kernphysik, TH Darmstadt
Gollerthan U, Brohm T, Clerc H G, Hanelt E, Horz M, Morawek W, Schwab W, Schmidt K H, Hessberger F P, Münzenberg G, Ninov V, Simon R S, Dufour J P and Montoya M 1991 *Z. Phys.* A **338** 51–60
Goodman A L 1988 *Phys. Rev.* C **37** 2162–9
Govil I M, Huizenga J R, Schröder W U and Töke J 1987 *Phys. Lett.* **197B** 515–8
Grangé P and Weidenmüller H A 1980 *Phys. Lett.* **96B** 26–30
Grangé P, Jun-Qing L and Weidenmüller H A 1983 *Phys. Rev.* C **27** 2063–77
Gross D H E, Nayak R C and Satpathy L 1981 *Z. Phys.* A **299** 63–72
Grossjean M K and Feldmeier H 1985 *Nucl. Phys.* A **444** 113–32
Gundlach J H, Snover K A, Behr J A, Gossett C A, Kicinska-Habior M and Lesko K T 1990 *Phys. Rev. Lett.* **65** 2523–6
Halbert M L, Beene J R, Hensley D C, Honkauen K, Semhov T M, Abenante V, Sarantites D G and Li Z 1989 *Phys. Rev.* C **40** 2558–75
Hamilton J H, Hansen P G and Zganjar E F 1985 *Rep. Prog. Phys.* **48** 631–708
Hansen G and Jensen A S 1983 *Nucl. Phys.* A **406** 236–56
Häusser O, Witthuhn W, Alexander T K, McDonald A B, Milton J C D and Olin A 1973 *Phys. Rev. Lett.* **31** 323–6

Haustein P E 1988 *At. Data Nucl. Data Tables* **39** 185–393
Heisenberg W 1932 *Z. Phys.* 77 1–11
Hessberger F P, Münzenberg G, Hofmann S, Agarwal Y K, Poppensieker K, Reisdorf W, Schmidt K H, Schneider J R H, Schneider W F W, Schött H J, Armbruster P, Thuma B, Sahm C C and Vermeulen D 1985a *Z. Phys.* A **322** 557–66
Hessberger F P, Münzenberg G, Hofmann S, Reisdorf W, Schmidt K H, Schött H J, Armbruster P, Hingmann R, Thuma B and Vermeulen D 1985b *Z. Phys.* A **321** 317–27
Hill D L and Wheeler J A 1953 *Phys. Rev.* **89** 1102–45
Hinde D J, Ogata H, Hanaha M, Shimoda T, Takahashi N, Shinohara A, Wahamatsu S, Katori K, Okamara H 1989 *Phys. Rev.* C **39** 2268–84
Hodgson P E 1987 *Rep. Prog. Phys.* **50** 1171–228
Hofmann S, Münzenberg G, Hessberger F and Schött H J 1984 *Nucl. Instrum. Methods* **223** 312–8
Hofmann H and Samhammer R 1985 *Z. Phys.* A **322** 157–62
Huizenga J R, Moretto L G 1972 *Ann. Rev. Nucl. Sci.* **22** 427–64
Ignatyuk A V, Istekov K K and Smirenkin G N 1979 *Yad. Fiz.* **30** 1205–18 (*Sov. J. Nucl. Phys.* **30** 626–33)
—— 1980 *Yad. Fiz.* **32** 347–54 (*Sov. J. Nucl. Phys.* **32** 180–4)
—— 1983 *Yad. Fiz.* **37** 831–8 (*Sov. J. Nucl. Phys.* **37** 495–9)
Ignatyuk A V, Itkis M G, Okolovich V N, Rus'kina G R, Smirenkin G N and Tishin A S 1977 *Yad. Fiz.* **25** 25–35 (*Sov. J. Nucl. Phys.* **25** 13–8)
Ignatyuk A V, Smirenkin G N and Tishin A S 1975 *Yad. Fiz.* **21** 485–90 (*Sov. J. Nucl. Phys.* **21** 255–7)
Inui M and Koonin S E 1984 *Phys. Rev.* C **30** 175–83
Iwamoto A 1987 *Phys. Rev.* C **35** 984–93
Jahnke U, Rossner H H, Hilscher D and Holub E 1982 *Phys. Rev. Lett.* **48** 17–20
Karwowski H J, Vigdor S E, Jacobs W W, Kalias S, Singh P P, Soga F, Throwe T G, Ward T E, Wark D L and Wiggins J 1982 *Phys. Rev.* C **25** 1355–78
Keller H, Lützenkirchen K, Kratz J V, Wirth G, Brüchle W and Sümmerer K 1987 *Z. Phys.* A **326** 313–26
Keller J G 1985 *PhD Thesis* Inst. Kernphysik, TH Darmstadt
Keller J G, Clerc H G, Schmidt K H, Agarwal Y K, Hessberger F P, Hingmann R, Münzenberg G, Reisdorf W and Sahm C C 1983 *Z. Phys.* A **311** 243–4
Keller J G, Schmidt K H, Hessberger F, Münzenberg G, Reisdorf W, Clerc H G and Sahm C C 1986 *Nucl. Phys.* A **452** 173–204
Keller J G, Schmidt K H, Stelzer H, Reisdorf W, Agarwal Y K, Hessberger F P, Münzenberg G, Clerc H G and Sahm C C 1984 *Phys. Rev.* C **29** 1569–71
Knox W J, Quinton A R and Anderson C E 1960 *Phys. Rev.* **120** 2120–8
Kramers H A 1940 *Physica* **7** 284–304
Krappe H J, Nix J R and Sierk A J 1979 *Phys. Rev.* C **20** 992–1013
Krappe H J, Möhring K, Nemes M C and Rossner H 1983 *Z. Phys.* A **314** 23–31
Kratz J V 1985 *Radiochim. Acta* **32** 25–41
Kühn W, Ruckelshausen A, Fischer R D, Breitbach G, Hennrich H J, Metag V, Novotny R, Jannssens R V F, Khoo T L, Habs D, Schwalm D, Haas B and Simon R S 1989 *Phys. Rev. Lett.* **62** 1103–5
Lacey R, Ajitanand N N, Alexander J M, de Castro Rizzo D M, De Young P, Kaplan M, Kowalski L, La Rana G, Logan D, Moses D J, Parker W E, Peaslee G F and Vaz L C 1987 *Phys. Lett.* **191B** 253–6
Lacey R, Ajitanand N N, Alexander J M, de Castro Rizzo D M, Peaslee G F, Vaz L C, Kaplan M, Kildir M, La Rana G, Moses D J, Parker W E, Logan D, Zisman M S, De Young P and Kowalski L 1988 *Phys. Rev.* C **37** 2540–60, 2561–77
Landowne S and Dasso C H 1984 *Phys. Lett.* **138B** 32–4
Landowne S and Pieper S C 1984 *Phys. Rev.* C **29** 1352–7
La Rana G, Moses D J, Parker W E, Kaplan M, Logan D, Lacey R, Alexander J M and Welberry R J 1987 *Phys. Rev.* C **35** 373–6
Lebrun C, Hanappe F, Lecolley J F, Lefebvres F, Ngô C, Péter J and Tamain B 1979 *Nucl. Phys.* A **321** 207–12
Leino M E, Yashita S and Ghiorso A 1981 *Phys. Rev.* C **24** 2370–3
Levinger J S 1960 *Nuclear Photo Disintegration* (London: Oxford University Press)
Levit S and Alhassid Y 1984 *Nucl. Phys.* A **413** 439–74
Liran S and Zeldes N 1976 *At. Data Nucl. Data Tables* **17** 431–41
Macfarlane R D and Griffioen R D 1963 *Nucl. Instrum. Methods* **24** 461–4
Maino G, Mengoni A, Ventura A 1990 *Phys. Rev.* C **42** 988–92
Mazarakis M G and Stephens W E 1973 *Phys. Rev.* C **7** 1280–7

McMahan M A and Alexander J M 1980 *Phys. Rev.* C **21** 1261–70
Meldner H 1967 *Ark. Fys.* **36** 593–8
Mignen J, Royer G and Sebille F 1988 *Nucl. Phys.* A **489** 461–76
Mohanty A K, Sastry S V S, Kataria S K and Ramamurthy V S 1990 *Phys. Rev. Lett.* **65** 1096–9
Möller P, Myers W D, Swiatecki W J and Treiner J 1988 *At. Data Nucl. Data Tables* **39** 225–33
Möller P and Nix J R 1981a *Nucl. Phys.* A **361** 117–46
—— 1981b *At. Data Nucl. Data Tables* **26** 165–96
—— 1988 *At. Data Nucl. Data Tables* **39** 213–23
Morawek W 1991 *PhD Thesis* Inst. Kernphysik, TH Darmstadt in preparation
Moretto L G 1972a *Nucl. Phys.* A **182** 641–68
—— 1972b *Nucl. Phys.* A **185** 145–65
—— 1974 *Proc. Symp. Phys. Chem. of Fission, Rochester 1973* vol 1 (Vienna: IAEA) pp 329–65
Moretto L G and Stella R 1970 *Phys. Lett.* **32B** 558–60
Moretto L G, Thompson S G, Routti J and Gatti R C 1972 *Phys. Lett.* **38B** 471–4
Mosel U and Greiner W 1969 *Z. Phys.* **222** 261–82
Moses D J, Kaplan M, Alexander J M, Logan D, Kildir M, Vaz L C, Ajitanand N N, Duek E and Zisman M 1985 *Z. Phys.* A **320** 229–36
Moses D J, Kaplan M, La Rana G, Parker W E, Lacey R and Alexander J M 1987 *Phys. Rev.* C **36** 422–4
Münzenberg G 1988 *Rep. Prog. Phys.* **51** 57–104
Münzenberg G, Armbruster P, Folger H, Hessberger F P, Hofmann S, Keller J, Poppensieker K, Reisdorf W, Schmidt K H and Schött H J 1984a *Z. Phys.* A **317** 235–6
Münzenberg G, Faust W, Hofmann S, Armbruster P, Güttner K and Ewald H 1979 *Nucl. Instrum. Methods* **161** 65–82
Münzenberg G, Hofmann S, Folger H, Hessberger F P, Keller J, Poppensieker K, Quint B, Reisdorf W, Schmidt K H, Schött H J, Armbruster P, Leino M E and Hingmann R 1985 *Z. Phys.* A **322** 227–35
Münzenberg G, Hofmann S, Hessberger F P, Folger H, Ninov V, Poppensieker K, Quint A B, Reisdorf W, Schött H J, Sümmerer K, Armbruster P, Leino M E, Ackermann D, Gollerthan U, Hanelt E, Morawek W, Fujita Y, Schwab T and Türler A 1988 *Z. Phys.* A **330** 435–6
Münzenberg G, Hofmann S, Hessberger F P, Reisdorf W, Schmidt K H, Schneider J R H, Armbruster P, Sahm C C and Thuma B 1981 *Z. Phys.* A **300** 107–8
Münzenberg G, Reisdorf W, Hofmann S, Agarwal Y K, Hessberger F P, Poppensieker K, Schneider J R H, Schneider W F W, Schmidt K H, Schmött H J, Armbruster P, Sahm C C and Vermeulen D 1984b *Z. Phys.* A **315** 145–58
Myers W D 1977 *Droplet Model of Atomic Nuclei* (New York: IFI/Plenum)
Myers W D and Schmidt K H 1983 *Nucl. Phys.* A **410** 61–73
Myers W D and Swiatecki W J 1966 *Nucl. Phys.* 81 1–60
—— 1967 *Ark. Fys.* **36** 343–52
—— 1969 *Ann. Phys., NY* **55** 395–505
—— 1974 *Ann. Phys., NY* **84** 186–210
Myers W D, Swiatecki W J, Kodama T, El-Jaick L J and Hilf E R 1977 *Phys. Rev.* C **15** 2032–43
Nebbia G, Nagel K, Fabris D, Majka Z, Natowitz J B, Schmitt R P, Sterling B, Mouchaty G, Berkowitz G and Strozewski K 1986 *Phys. Lett.* **176B** 20–5
Nilsson S G, Tsang C F, Sobiczewski A, Szymanski Z, Wycech S, Gustafson C, Lamm I L, Möller P and Nilsson B 1969 *Nucl. Phys.* A **131** 1–66
Nitschke J M, Leber J R, Nurmia J J and Ghiorso A 1979 *Nucl. Phys.* A **313** 236–50
Nix J R and Sierk A J 1977 *Phys. Rev.* C **15** 2072–82
Oganessian Yu Ts 1974 *Lecture Notes in Physics* **33** (Berlin: Springer) pp 221–52
—— 1988 *Nucl. Phys.* A **488** 65c–82c
Oganessian Yu Ts, Demin A G, Ilj A S, Tretya S P, Pleve A A, Penionzhkevich Y E, Ivanov MP and Tretyakov Y P 1975 *Nucl. Phys.* A **239** 157–71
Oganessian Yu Ts, Hussonnois M, Demin A G, Kharitonow Yu P, Bruchertseifer H, Constantinescu O, Korotkin Yu S, Tretyakova S P, Utyonkow V K, Shirokovsky I V and Estevez J 1984 *Radiochim. Acta* **37** 113–20
Orlova O A, Bruchertseifer H, Muzychka Yu A, Oganesyan Yu Ts, Pustylnik B F, Ter-Akopian G M, Chepigin V I and Choy Vol Sek 1978 *Internal Report JINR, Dubna* P7-12061
Patterson J R, Nagorcka B N, Symons G D and Zuk W M 1971 *Nucl. Phys.* A **165** 545–59
Patyk Z and Sobiczewski A 1990 *Gesellschaft für Schwerionenforschung, Darmstadt Preprint* GSI-90-53
Patyk Z, Sobiczewski A, Armbruster P and Schmidt K H 1988 *Nucl. Phys.* A **491** 267–80

Pengo R, Evers D, Löbner K E G, Quade U, Rudolph K, Skorka S J and Weidel I 1983 *Nucl. Phys.* A **411** 255–74

Quint A B, Schmidt K H, Reisdorf W, Armbruster P, Hessberger F P, Keller J G, Münzenberg G, Stelzer H, Clerc H G, Morawek W and Sahm C C 1991 to be published

Ramamurthy V S, Mohanty A K, Kataria S K and Rangarajan G 1990 *Phys. Rev.* C **41** 2702–7

Rehm K E, Wolfs F L H, van den Berg A M, Henning W 1985 *Phys. Rev. Lett.* **55** 280–3

Reisdorf W 1981 *Z. Phys.* A **300** 227–38

—— 1986 *Proc. Int. Conf. on Nuclear Physics, Harrogate, August 1986 (Inst. Phys. Conf. Ser.* **86**) (Bristol: Hilger) pp 205–25

—— 1988 *Lecture Notes in Physics* **317** (Berlin: Springer) pp 26–39

Reisdorf W, Hessberger F P, Hildenbrand K D, Hofmann S, Kratz J V, Münzenberg G, Schlitt K, Schmidt K H, Schneider J H R, Schneider W F W, Sümmerer K and Wirth G 1982 *Phys. Rev. Lett.* **49** 1811–5

Reisdorf W, Hessberger F P, Hildenbrand K D, Hofmann S, Münzenberg G, Schmidt K H, Schneider J H R, Schneider W F W, Sümmerer K, Wirth G, Kratz J V, Schlitt K 1985a *Nucl. Phys.* A **438** 212–52

Reisdorf W, Hessberger F P, Hildenbrand K D, Hofmann S, Münzenberg G, Schmidt K H, Schneider J H R, Schneider W F W, Sümmerer K, Wirth G, Kratz J V, Schlitt K and Sahm C C 1985b *Nucl. Phys.* A **444** 154–88

Rivet M F, Alami R, Borderie B, Fuchs H, Gardes D and Gauvin H 1988 *Z. Phys.* A **330** 295–301

Rivet M V, Logan D, Alexander J M, Guerreau D, Duek E, Zisman M and Kaplan M 1982 *Phys. Rev.* C **25** 2430–49

Rost E 1968 *Phys. Lett.* **26B** 184–7

Rowley N, Kabir A, Lindsay R 1989 *J. Phys. G: Nucl. Part. Phys.* **15** L269–75

Royer G, Piller C, Mignen J and Raffray Y 1990 *J. Phys. G: Nucl. Part. Phys.* **16** 1077–88

Rudolph K, Evers D, Konrad P, Löbner K E G, Quade U, Skorka S J and Weidl I 1983 *Nucl. Instrum. Methods* **204** 407–18

Sahm C C, Clerc H G, Schmidt K H, Reisdorf W, Armbruster P, Hessberger F P, Keller J G, Münzenberg G and Vermeulen D 1984 *Z. Phys.* A **319** 113–8

—— 1985 *Nucl. Phys.* A **441** 316–43

Sahm C C, Schulte H, Vermeulen D, Keller J, Clerc H G, Schmidt K H, Hessberger F and Münzenberg G 1980 *Z. Phys.* A **297** 241–5

Salomaa M and Enge H A 1977 *Nucl. Instrum. Methods* **145** 279–82

Sandorfi A M 1984 *Treatise on Heavy-Ion Science* vol 2, ed D A Bromley (New York: Plenum) pp 53–111

Schmidt K H, Delagrange H, Dufour J P, Cârjan N, Fleury A 1982 *Z. Phys.* A **308** 215–25

Schmidt K H, Faust W, Münzenberg G, Clerc H G, Lang W, Pielenz K, Vermeulen D, Wohlfarth H, Ewald H and Güttner K 1979 *Nucl. Phys.* A **318** 253–68

Schmidt K H, Faust W, Münzenberg G, Reisdorf W, Clerc H G, Vermeulen D and Lang W 1980 *Proc. Symp. Physics and Chemistry of Fission, Jülich, 1979* vol 1 (Vienna: IAEA) pp 409–20

Schmidt K H, Keller J G and Vermeulen D 1984a *Z. Phys.* A **315** 159–62

Schmidt K H, Sahm C C, Pielenz K and Clerc H G 1984b *Z. Phys.* A **316** 19–26

Schmidt K H, Simon R S, Keller J G, Hessberger F P, Münzenberg G, Quint B, Clerc H G, Schwab W, Gollerthan U and Sahm C C 1986 *Phys. Lett.* **168B** 39–42

Schmidt K H and Vermeulen D 1980 *Atomic Masses and Fundamental Constants* 6 ed J A Nolen and W Benenson (New York: Plenum) pp 119–28

Seaborg G T and Loveland W D 1985 *Treatise on Heavy Ion Science* ed D A Bromley (New York: Plenum) pp 255–330

—— 1990 *The Elements beyond Uranium* (New York: Wiley)

Shen W Q, Albinski J, Gobbi A, Gralla S, Hildenbrand K D, Herrmann N, Kuzminski O, Müller W F J, Stelzer H, Tõke J, Back B B, Bjørnholm S and Sørensen S P 1987 *Phys. Rev.* C **36** 115–42

Sierk A J 1986 *Phys. Rev.* C **33** 2039–53

Sierk A J and Nix J R 1974 *Proc. Symp. Physics and Chemistry of Fission, Rochester, 1973* vol 2 (Vienna: IAEA) pp 273–87

Skorka S J, Stefanini A M, Fortuna G, Pengo R, Meczynski W, Beghini S, Signorini C and Pascholati P R 1987 *Z. Phys.* A **328** 355–62

Snover K A 1986 *Ann. Rev. Nucl. Part. Sci.* **36** 545–603

—— 1988 *Nucl. Phys.* A **482** 13c–26c

Stefanini A M, Fortuno G, Pengo R, Meczynski W, Montagnoli G, Corradi L, Tirelli A, Beghini S, Signorini C, Lunardi S, Morando M and Soramel F 1986 *Nucl. Phys.* A **456** 509–34

Stokstad R G 1984 *Treastise on Heavy-Ion Science* vol 3, ed D A Bromley (New York: Plenum) pp 83–197

Stokstad R G, Di Gregorio D E, Lesko K T, Harmon B A, Norman E B, Pouliot J and Chan Y D 1989 *Phys. Rev. Lett.* **62** 399–402
Stokstad R G, Eisen Y, Kaplanis S, Pelte D, Smilansky U and Tserruya I 1978 *Phys. Rev. Lett.* **41** 465–9
—— 1980a *Phys. Rev.* C **21** 2427–35
Stokstad R G, Reisdorf W, Hildenbrand K D, Kratz J V, Wirth G, Lucas R and Poitou J 1980b *Z. Phys.* A **295** 269–86
Strutinsky V M 1967 *Nucl. Phys.* A **95** 420–42
Sujkowski Z, Balster G J, Chmielewska D and Wilschut H W 1983 *Phys. Lett.* **133B** 53–6
Swiatecki W J 1956 *Phys. Rev.* **101** 97–9
—— 1980 *Prog. Part. Nucl. Phys.* **4** 383–450
—— 1981 *Phys. Scr.* **24** 113–22
—— 1982 *Nucl. Phys.* A **376** 275–91
—— 1983 *Aust. J. Phys.* **36** 641–8
Switkowski Z E, Stokstad R G and Wieland R M 1976 *Nucl. Phys.* A **274** 202–22
Tachibana T, Uno M, Yamada M. and Yamada S 1988 *At. Data Nucl. Data Tables* **39** 251–8
Tōke J and Swiatecki W J 1981 *Nucl. Phys.* A **372** 141–50
Tōke J, Bock R, Dai G X, Gobbi A, Gralla S, Hildenbrand K D, Kuzminski J, Müller W F J, Olmi A, Stelzer H, Back B B and Bjørnholm S 1985 *Nucl. Phys.* A **440** 327–65
Vandenbosch R and Huizenga J R 1973 *Nuclear Fission* (New York: Academic)
Vandenbosch R, Murakami T, Sahm C C, Leach D D, Ray A and Murphy M J 1986 *Phys. Rev. Lett.* **56** 1234–6
Vandenbosch R and Seaborg G T 1958 *Phys. Rev.* **110** 507–13
Vaz L C and Alexander J M 1984 *Z. Phys.* A **318** 231–7
Vaz L C, Alexander J M and Satchler G R 1981 *Phys. Rep.* **69** 373–99
Vermeulen D, Clerc H G, Sahm C C, Schmidt K H, Keller J G, Münzenberg G and Reisdorf W 1984 *Z. Phys.* A **318** 157–69
Vigdor S E and Karwowski H J 1982 *Phys. Rev.* C **26** 1068–88
Wapstra A H, Audi G and Hoekstra R 1988 *At. Data Nucl. Data Tables* **39** 281–7
Weißkopf V F 1937 *Phys. Rev.* **52** 295–303
Will C M and Guinn J W 1988 *Phys. Rev.* A **37** 3674–9
Wong C Y 1973 *Phys. Rev. Lett.* **31** 766–9
Wu S C, Overley J C, Barnes C A and Switkowski Z E 1978 *Nucl. Phys.* A **312** 177–200
Yeremin A V, Andreyev A N, Bogdanow D D, Chepigin V I, Gorshkov V A, Ivanenko A I, Kabachenko A P, Rubinskaya L A, Smirnova E M, Stepantsov S V, Voronkov A N and Ter-Akopian G M 1989 *Nucl. Instrum. Methods* A **274** 528–32
Zeldes M, Dumitresku T S and Koehler H S 1983 *Nucl. Phys.* A **399** 11–50